# *Parabacteroides distasonis* enhances Type 1 Diabetes autoimmunity via molecular mimicry

Qian Huang[1], I-Ting Chow[2], Claudia Brady[1], Amol Raisingani[1], Danmeng Li[3], David A. Ostrov[3], Mark A. Atkinson[3,4], William W. Kwok[2], C. Ronald Kahn[5], Emrah Altindis[1]*

[1] Boston College Biology Department, Higgins Hall, 140 Commonwealth Avenue Chestnut Hill, MA 02467, USA

[2] Benaroya Research Institute at Virginia Mason, Seattle, WA 98101, USA

[3] Department of Pathology, Immunology and Laboratory Medicine, College of Medicine, University of Florida Diabetes Institute, Gainesville, FL 32610-3633, USA

[4] Department of Pediatrics, College of Medicine, University of Florida Diabetes Institute, Gainesville, FL 32610-3633, USA

[5] Joslin Diabetes Center, Harvard Medical School, Boston, MA, 02215, USA

***Corresponding Author:** Emrah Altindis, Boston College Biology Department, Higgins Hall, 140 Commonwealth Avenue Chestnut Hill, MA 02467. E-mail: altindis@bc.edu

**One Sentence Summary:** The human gut commensal bacterium, *Parabacteroides distasonis*, accelerates type 1 diabetes in the NOD mouse model of the disease and involves expression of an insulin B:9-23 epitope mimic, supporting a potential disease mechanism involving molecular mimicry.

## ABSTRACT

Type 1 Diabetes (T1D) is an autoimmune disease characterized by destruction of pancreatic β-cells. Focusing on the main insulin epitope, insulin B-chain 9-23 (insB:9-23), we explored whether a microbial insB:9-23 mimic could modulate T1D. We now demonstrate that a microbial insB:9-23 mimic of *Parabacteroides distasonis*, a human gut commensal, exclusively stimulates non-obese diabetic (NOD) mouse T cells specific to insB:9-23. Indeed, immunization of NOD mice with either the bacterial mimic peptide or insB:9-23 further verified the cross-reactivity in vivo. Modeling *P. distasonis* peptide revealed a potential pathogenic register 3 binding. *P. distasonis* colonization of the female NOD mice gut accelerated T1D onset. In addition, adoptive transfer of splenocytes from NOD mice colonized with *P. distasonis* to NOD.SCID recipients conferred the enhanced disease phenotype. Integration analysis of published infant T1D gut microbiome data revealed that *P. distasonis* peptide is not present in the gut microbiota in the first year of life of infants that eventually develop T1D. Furthermore, *P. distasonis* peptide can stimulate human T cell clones specific to insB:9-23 and T1D patients demonstrated a strong humoral immune response to *P. distasonis* than controls. Taken together, our studies define a potential molecular mimicry link between T1D pathogenesis and the gut microbiota.

## INTRODUCTION

Type 1 diabetes (T1D) is an autoimmune disease characterized by selective destruction of pancreatic β-cells by autoreactive T cells (1). The incidence rate of T1D in children is rising on an annual basis both in Europe (3.4 %) and the USA (1.4 %) (2, 3). Genome-wide association studies (GWAS) have identified ~50 genetic regions that influence the risk of developing T1D, but genetics alone cannot account for the increasing incidence rates of T1D. For example, incidence rates of T1D in two neighboring regions, Russian Karelia and Finnish Karelia are six-fold different; despite a very similar genetic background of the inhabitants (4). Furthermore, even among identical twins, the concordance of T1D is only 40-60% (5, 6). Various environmental factors have been studied including diet, birth mode, infections and antibiotics; however, the roles of these factors and cause of T1D largely remain unknown (7-9). This said, recent gut microbiome studies have observed an altered microbial and metabolite composition, and increased intestinal permeability in subjects with T1D (10-14). In addition to gut microbes, viral infections have also been suggested to play a role in T1D, yet no studies have identified a direct causal link (15). Taken together, these data suggest that genetics alone cannot explain the risk of T1D autoimmunity.

One of the earliest markers of T1D autoimmunity is the development of islet autoantibodies against insulin (IAA), glutamic acid decarboxylase (GADA), insulinoma-associated autoantigen 2 (IA-2A), zinc transporter 8 (ZnT8A) and islet specific glucose-6-phosphatase catalytic subunit related protein (IGRP, recently named G6PC2) (16, 17). Among these, insulin is the only autoantigen exclusively expressed by β-cells, with IAA usually the first to be detected (18, 19). In humans, IAA develop months to years before the onset of overt diabetes (20), and, there is a significant correlation between IAA concentration and rate of progression to T1D (21). In addition to humoral immune responses, insulin is a target of $CD4^+$ T cells in both humans and murine

autoimmune diabetes. In theNOD mouse model of T1D (22), over 90% of the anti-insulin $CD4^+$ T cell clones target amino acids 9-23 of the insulin B chain (insB:9-23) (23). Importantly, InsB:9-23 specific T-cells have also been identified in islets obtained from human organ donors with T1D (24, 25) as well as in peripheral blood lymphocytes of living T1D patients (19, 26, 27). Clearly lacking in this field are studies that have the ability to pull together such findings and, bring together a central hypothesis for testing of a strong, well supported, central hypothesis.

In this regard, the concept of molecular mimicry has long been noted as a potential trigger for autoimmunity; one when the immune response cannot discriminate a foreign antigen from a self-protein (8, 28). In this study, we hypothesized that exposure to a microbial insulin epitope mimic could stimulate an autoimmune response initiating T1D onset. To address this question, we screened for microbial mimics of insB:9-23 and subsequently evaluated one such mimic from a gut commensal, *Parabacteroides distasonis*; this, for the notion of stimulating insB:9-23-specific human and NOD T cells ex vivo as well as to modulate T1D progression in vivo. We also leveraged existing human gut microbiota datasets from the BABYDIET and DIABIMMUNE studies to explore microbial colonization and expression of insB:9-23 mimics during the first years of life in children who later developed T1D. Taken together, our studies demonstrated that insulin epitope mimics in the gut microbiota may play an important role in T1D onset ,via a molecular mimicry mechanism, particularly when exposed after the neonatal period of immune development.

## RESULTS

### *Parabacteroides distasonis* insB:9-23 like peptide cross-reacts with NOD mouse T cell hybridomas specific to insB:9-23

To test our aforementioned molecular mimicry hypothesis, we focused on the dominant T-cell epitope, insB:9-23. We first identified microbial insB:9-23 peptide mimics, searching the NCBI databases for viral (taxid:10239), bacterial (taxid:2) and fungal (taxid:4751) proteomes using the insB:9-23 sequence (SHLVEALYLVCGERG) as the query sequence. We identified 47 microbial peptides with over eight residues identical with the insulin peptide (**Table S1**). Among these microbial mimics, 17 bacterial and viral mimics contained the previously identified residues in the insB:9-23 critical for binding to the NOD MHC I-$A^{g7}$ and human HLA-DQ2-8 molecule (**Table 1**). To test whether microbial insB:9-23 mimics can stimulate NOD T cells, we used IIT3 and 8F10 T cell hybridomas. IIT3 recognizes presented insulin protein as well as the insB:9-23 peptide, whereas 8F10 recognizes only the insB:9-23 peptide (29). We also used a C3g7 cell line expressing a large amount of I-$A^{g7}$, as antigen presenting cells (APCs). Among the 17 microbial peptides tested, only one stimulated IIT-3 hybridomas (**Figure 1A**). This peptide contained in the N-terminal of the hypoxanthine phosphoribosyltransferase (hpt) protein of *P. distasonis 33B* formerly known as *Bacteroides sp. 2_1_33B (30)* (**Figure S1A**). Yang et al. recently demonstrated that residues from insB:15-20 are essential to stimulate the human T cell clones via register 3 (27). Indeed, the *P. distasonis* peptide is the only tested microbial mimic that has all six residues conserved in this region (**Table 1, S1**). Notably, *P. distasonis* 33B and D13 strains are the only organisms that possess this unique insB:9-23 mimic sequence in their genomes in the NCBI dataset (as of September 12, 2020, **Figure S1B-C, Supplementary Document 1-2**). Taken together, as a

member of the human gut microbiome, *P. distasonis* makes an interesting candidate for T1D autoimmunity.

With these results, we repeated the T cell hybridoma stimulation experiment using *P. distasonis* lysate or growth culture instead of the 15-mer peptide, but did not observe a robust response (**Figure S3A-B**). However, it is well known that some bacterial proteins are not expressed in vitro and require specific conditions mimicking in vivo (31). Indeed, using RT-qPCR, we observed extremely low gene expression of Hpt in our *P. distasonis* culture (**Figure S3C**). Moreover, we performed an SDS-PAGE gel of the bacterial lysate and analyzed all bands between 20 and 50 kDa. *P. distasonis* Hpt protein, which is predicted to be 27.3 kDa, was not identified among the 464 proteins detected by liquid chromatography-mass spectrometry (LC-MS) MS analysis (**Table S2**).

**Structural modeling of *P. distasonis* insB:9-23-like peptide suggests potential binding to MHC in a specific register.**

Previous studies have demonstrated the importance of specific insB:9-23 peptide positions in anchoring the peptide to the MHC binding cleft in a manner that determines the binding register (32). To understand the molecular mechanism underlying such cross-reactivity, we developed an in silico model of the *P. distasonis* peptide compared to the native insB:9-23 epitope (**Figure 1B, S2**). Glutamic acid at position 9 (P9) of insB:9-23 confers binding in "register 2", whereas non-glutamic acid side chains, such as arginine, impose peptide binding in "register 3"(32). Variants of insB:9-23 presented in register 3 elicit stronger autoreactive T cell responses compared to insB:9-23 presented in register 2. In the context of register 3, the *P. distasonis* mimic and insB:9-23 peptide share a high degree of sequence homology except at P9. The *P. distasonis* mimic

peptide has a tyrosine (Y) at P9 versus serine (S) in the native insulin epitope, whereas most of the other microbial mimics have an arginine (R) at P9, which is not expected to shift the register. The binding model of insB:9-23 and *P. distasonis* peptide revealed that the *P. distasonis* mimic peptide has the potential to bind MHC in register 3, thus resulting in presentation of peptide side chains that are identical between insB:9-23 and *P. distasonis* (**Figure 1B, S2A-B**). These data support our observation that T cells responding to the register 3 bound insulin peptide have the ability to cross react with the *P. distasonis* peptide in register 3 (**Figure 1A**).

**Immunization of NOD mice with *P. distasonis* peptide stimulates cross-reactive T-cells**

To further explore this peptide cross-reactivity, we immunized NOD mice with either (i) insB:9-23 peptide or, (ii) *P. distasonis* mimic peptide with Complete Freund's Adjuvant (CFA). After 7 days, we collected the popliteal lymph nodes and examined T cell activity by enzyme-linked immunospot (ELISpot) for interferon-gamma (IFNg) and IL-2 secretion; this, following *in vitro* stimulation with either the insB9-23 or microbial mimic peptide. Immunization of mice with the *P. distasonis* peptide generated a cross-reactive immune response to insB9-23 (**Figure 1C and 1E**). Likewise, immunization of mice with insB:9-23 stimulated a cross-reactive response to the *P. distasonis* peptide, which was even stronger than the stimulation with the insulin peptide (**Figure 1D and 1F**).

***P. distasonis* colonization accelerates diabetes onset in female NOD mice**

Based on our findings on cross-reactivity, we hypothesized that *P. distasonis* colonization and exposure to the microbial insB:9-23 mimic can trigger the immune response and stimulate autoimmunity in NOD mice. To test this hypothesis, we orally gavaged both male and female

NOD mice with *P. distasonis* ($10^{9}$ **CFU** *P. distasonis*/mouse/day) or saline daily after weaning, starting at 3 weeks of age (**Figure 2A**, n=40/group). Neither male nor female NOD mice carried *P. distasonis* in their gut under specific pathogen free (SPF) housing conditions (**Figure 2B**), providing an ideal control to determine the effect of the *P. distasonis* colonization on T1D onset. After 30 days of oral gavage, we detected colonization of the gut with *P. distasonis* (**Figure 2B**). At 12 weeks of age (pre-diabetic), we randomly separated five mice from each group and collected the pancreas for immunostaining. Interestingly, the *P. distasonis* colonized female NOD mice showed significantly higher insulitis scores as compared to controls (**Fig 2C, Fig S4A representative figures**). Moreover, *P. distasonis* colonization significantly accelerated T1D onset in female NOD mice (survival: 42% versus 19.5%) (**Figure 2D**). This effect was specific to the female mice as no differences in insulitis or T1D incidence were observed in male mice administered *P. distasonis* versus saline (**Figure 2C-D**).

**_P. distasonis_ stimulates a specific humoral immune response in colonized NOD mice.**

To determine whether *P. distasonis* colonization can stimulate IAA seroconversion, we measured IAA levels with ELISA at 12 weeks of age in study animals. Only a small fraction of the mice had circulating IAA at this early point, with no significant differences between study groups detected (**Fig. S4B**). Western blot analysis using plasma samples obtained from the same NOD mice (12 weeks) revealed that *P. distasonis* colonization stimulated a very strong humoral immune response to the bacterium in both female and male NOD mice (**Figure 2E-F**). To evaluate the specificity of this humoral response, we performed a similar Western blot using the plasma samples to detect lysates from another well studied gut commensal, *Bacteroides fragilis*, that was shown to have

175 immunomodulatory effects in NOD mice *(33)*. As expected, we detected a weak humoral immune
176 response to *B. fragilis* lysates in both the saline and *P. distasonis* treated groups (**Figure S4C-D**).
177 Serum LPS levels were not significantly different between the groups indicating that this *P.*
178 *distasonis* specific humoral response did not result from gut barrier dysfunction (leaky gut)
179 stimulated by *P. distasonis* colonization (**Figure 2G**). We measured multiple (n=32) serum
180 cytokines and chemokines using a multiplex Luminex assay (Millipore) to determine whether *P.*
181 *distasonis* colonization of the female NOD mice alters the systemic immune response but did not
182 detect any differences between the two groups (**Table S3**). These results suggest that *P. distasonis*
183 stimulates a specific immune response but not IAA or elevated proinflammatory cytokines.

184 **Adoptive transfer of splenocytes enhance T1D onset in immunodeficient NOD.SCID mice**

185 We next performed an adoptive transfer experiment (**Figure 3A**) using immunodeficient
186 NOD.SCID mice, which lack functional B or T cells, as recipients (34). We orally gavaged a new
187 cohort of the NOD mice with *P. distasonis* or saline (n=16-20/group) as described above and
188 transferred $5x10^7$ splenocytes from individual NOD donor mice to 6 week old NOD.SCID
189 recipients (1:1 ratio, sex-matched, n=16-20 per group) (**Figure 3B**). Consistent with the
190 spontaneous T1D experiment (**Figure 2D**), recipient female NOD.SCID mice that received
191 splenocytes from the *P. distasonis* treated group developed T1D at a significantly higher rate
192 (**Figure 3C**). Thus, an adaptive immune response stimulated by *P. distasonis* exposure in female
193 NOD mice is sufficient to transfer and accelerate T1D.

194

195 **Subcutaneous injection of *P. distasonis* peptide is protective in female NOD mice**

Subcutaneous injection of mouse insulin 2, B:9-23 into female NOD mice for 25 weeks was shown to be protective in female NOD mice, with this result explained by a T helper 2 (Th2) cell shift in immune response (35). To determine whether a different route of *P. distasonis* peptide administration is protective, we injected female (n=20/peptide) and male (n=20/peptide) NOD mice with i) insB:9-23 insulin 2, ii) the *P. distasonis* B:9-23 mimic, iii) saline (vector), or iv) tetanus toxoid (TT) control peptide weekly for 20 weeks beginning at 4 weeks of age. Consistent with the oral gavage experiments (**Figures 2D and 3C**), we did not observe any effect of *P. distasonis* B:9-23 peptide on male NOD mice (**Figure 3D**) while insB:9-23 and the *P. distasonis* peptide significantly delayed T1D onset in female NOD mice (**Figure 3E**). This further confirms the cross reactivity between insB:9-23 and the *P. distasonis* peptide mimic, but the route of exposure (i.e., subcutaneous versus mucosal) appears to impact the ability to modulate T1D onset (**Figure 2D and 3E**).

## ***P. distasonis* B:9-23 like peptide is not present in the gut microbiota of children developing T1D in the first year of life.**

To investigate a potential role for the *P. distasonis* insB:9-23 mimic in human T1D, we analyzed published human gut microbiome data emanating from the BABYDIET study, where 16S Illumina sequencing was used to analyze stool samples collected from 22 children who developed islet autoantibodies, with 10 developing diabetes after a median follow-up time of 5 years, as well as from 22 healthy subjects from birth to 3 years of age (36). We searched for the operational taxonomic units (OTUs) identified as *P. distasonis* and classified the data according to sample collection time (0-1, 1-2 and 2-3 years of age) and subject disease status at the end of the study

(control, autoantibody (Ab) positive, or T1D). *P. distasonis* was present in control children at all three time points, but was only identified in the second year of age and later in the children who developed T1D. Moreover, compared to controls, fewer *P. distasonis* OTUs were identified for the first year in the 12 children who developed autoantibodies but did not progress to T1D during follow-up (**Figure 4A**). A key limitation of this 16S rRNA gene sequencing data is the inability to determine whether the identified *P. distasonis* OTUs carry the insulin B9-23 mimic peptide.

To address this, we next analyzed published DIABIMMUNE metagenomic data obtained from three countries: Russia, Finland and Estonia (11). In this study, researchers performed shotgun metagenomics sequencing on stool samples collected annually from genetically predisposed subjects from birth to age 3 years in Finland, Russia and Estonia (n=74/country). To identify optimized alignments, we first assembled the contigs and searched for DNA sequences capable of encoding the *P. distasonis* peptide. Consistent with the BABYDIET results (**Figure 4A**), we were unable to identify the *P. distasonis* epitope mimic in the first year of life for subjects who later developed autoantibodies (seroconverted, Ab positive **Figure 4B**). We next analyzed the data stratified by country. While no subjects were exposed to the *P. distasonis* peptide in the first year of age, the peptide was identified in all subjects who develop autoantibodies in Estonia after age one and in Russia after age two. In contrast, the children who developed autoantibodies in Finland were never exposed to this peptide in the first three years of age; suggesting a potential later time point of exposure or a different trigger **(Fig. 4C)**. In sum, these results suggest that the late exposure to the *P. distasonis* insB:9-23 mimic in years 2-3 of childhood might trigger an immune response and stimulate autoimmunity. Indeed, these observations are consistent with our findings in NOD mice. Colonization of the gut microbiota with to *P. distasonis* after weaning, at a late time point relative to immune development, accelarated the disease in female NOD mice.

241 ***P. distasonis* peptide can stimulate insB:9-23 specific human T-cell clones**

242 To further characterize the immune response against *P. distasonis*, we investigated the humoral
243 response in human T1D patients to determine their exposure. Specifically, we tested antibody
244 responses using serum obtained from female subjects with T1D and age and ethnicity matched
245 controls (n=8/group, median age 16.2, median duration 4.3 years). Indeed, four of eight female
246 subjects with T1D demonstrated an elevated immune response to *P. distasonis* lysates compared
247 to the eight controls and other T1D four samples (**Figure 4D Table S4**). Because T1D is T-cell
248 mediated, we also tested whether the *P. distasonis* insB:9-23 mimic or 17 other insB:9-23 like
249 peptides (**Table 1**) could stimulate insB:11-23-specific T cell clones isolated from participant
250 T1D#3 in (27). The insB:9-23R$^{22E}$ peptide was previously shown to be more potent than insB:9-
251 23 in stimulating insB:9-23 hybridomas from NOD mice (32) and human T-cell clones (27); hence
252 we used both insB:9-23R$^{22E}$ and insB:9-23 as positive controls and a scrambled peptide as a
253 negative control (**Table 1**). Consistent with our findings with NOD mice hybridomas (**Figure 1**),
254 the *P. distasonis* peptide (peptide 1) was the only microbial peptide among 17 tested that could
255 stimulate human T cells to produce IFN-g (**Figure 4E, F**).
256
257

## DISCUSSION

There have been tremendous efforts to understand the triggers of T1D autoimmunity, however, the etiology of the disease is complex and remains incompletely characterized. In this study, we investigated molecular mimicry as a potential mechanism linking microbial flora to T1D onset. Molecular mimicry mechanisms are based on the degeneracy of T cell recognition (37, 38) and can be either pathogenic (39) or protective (40). While the molecular mimicry hypothesis was popular in T1D research in the 1990s (41-43), progress in this area is very limited in the last 20 years (44). In the current study, taking advantage of these growing genome databases, we identified candidate microbial mimic peptides for the T1D target epitope, insB:9-23. We further show that stimulation of the immune system with a gut commensal's, *P. distasonis,* insB:9-23 like peptide can stimulate an immune response to the endogenous insB:9-23. Moreover, exposure to *P. distasonis* during gut microbiota development caused increased infiltration to the islets and accelerated diabetes onset in female NOD mice. This pathogenic effect was mediated by splenocytes as evidenced by adoptive transfer to female NOD.SCID mice.

A plethora of human gut microbiome studies demonstrated that the composition of the gut microbiota of patients with autoimmune diseases including multiple sclerosis (45), systemic lupus erythematosus, anti-phospholipid syndrome (46), Crohn's disease (47-49), ulcerative colitis (50), inflammatory bowel diseases (51, 52), and coeliac disease (53) are significantly different from healthy controls. Although the methodologies and conclusions differ in microbiota studies from subjects with and at-risk for T1D (11-13, 54), there is a common pattern. Specifically, the diversity of T1D patients' gut microbiome is decreased while there is an increased prevalence of *Bacteriodetes* taxa and an altered metabolomic profile compared to healthy controls (14). Most of these studies are observational and do not define any mechanism related to T1D onset. One

exception is the DIABIMMUNE study (13) wherein authors concluded that the higher T1D rates in Finnish Karelia and Estonia compared to Russian Karelia might be related to the gut microbiota composition. They suggest that while Russian infants are exposed to *Escherichia coli* LPS, the Finnish and Estonian infants are exposed to *Bacteroides* species' LPS, which inhibits endotoxin tolerance. They also showed that injection of *E. coli* LPS protected NOD mice from developing T1D; however, they did not report any data validating the LPS hypothesis for human T1D.

As the largest human gut microbiome study collecting 12,005 samples from 903 children in four countries in seven locations, The Environmental Determinants of Diabetes in the Young (TEDDY) trial identified *Parabacteroides* as the most significantly associated genus with T1D (55). This is consistent with our findings related to *P. distasonis* mimic analysis from Russia and Estonia wherein 100% of the children developing T1D had the *P. distasonis* peptide in their gut microbiota in years 2-3 of life. The TEDDY study also recently showed that human gut microbiota development is divided in three phases: a developmental phase (months 3-14), a transitional phase (months 15-30), and a stable phase (months 31-46) (55). Using the DIABIMMUNE sequencing data, we showed that the *P. distasonis* insB:9-23 mimic peptide is not present in the gut microbiota during the developmental phase (i.e., the first year of life) in the children who go on to develop T1D. Our data suggest that the absence of *P. distasonis* in the developmental phase may be critical in T1D pathogenesis. A recent study showed that in addition to thymic education of the immune system for self-tolerance, the microbiota provides a post-thymic education to provide tolerance to commensal microbiota (56). Thus, the presence of the *P. distasonis* insB:9-23 mimic in this early stage might promote tolerance to the insulin epitope. Hence, there might be a window of opportunity for exposure during the developmental phase of gut microbiota development during which the *P. distasonis* peptide might stimulate regulatory T cells (Tregs) and immunotolerance

for insB:9-23. Although further studies are needed to investigate the direct link between human T1D and *P. distasonis*, the cross-reactivity of the insB:9-23 mimic with human T cell clones represents a clear potential mechanism. Furthermore, the strong humoral immune response to *P. distasonis* lysate clearly shows the exposure and humoral immune response in a fraction of T1D patients.

In addition to their critical role in NOD mouse diabetes onset (57), insB:9-23 specific $CD4^+$ T cells were identified in human islets (24, 25) and in peripheral blood of T1D patients (19, 26, 27). While our study is insB:9-23 centric, there are other epitopes recognized by human islet-infiltrating or circulating T-cells in insulin B-chain (58), A-chain (59, 60) or C-peptides (24, 25). A recent discovery showed that hybrid insulin peptides (HIPs) are novel epitopes formed with post-translational modifications formed in the beta cell granules (61-63). Likewise, defective ribosomal products (Drips) of insulin were shown to lead of aberrant insulin polypeptides rendering beta cells immunogenic (64). Babon et al. recently showed that $CD4^+$ and $CD8^+$ T cell lines or clones isolated from the islets of nine donors with T1D are stimulated by several islet antigens including GAD, insulin, IA-2 and HIPs (65). Given the enormous number of microbial peptides produced by the gut microbiota, we expect that others may exist with the potential to mimic these additional epitopes and trigger cognate autoantigen reactive T cells. Indeed, Tai et al. identified a microbial peptide mimic produced by *Fusobacteria* that can stimulate IGRP-specific mouse T cells and promote diabetes development in a new TLR-deficient ($TLR^{-/-}$) and $MyD88^{-/-}$ NY8.3 NOD mouse model (66).

Although gut microbiota has a critical role in modulating T1D onset in NOD mice (67), there are very few studies focusing on the effects of a single bacterium. For example, the presence of segmented filamentous bacteria correlated with protection in NOD mice (68). Likewise,

Hanninen et al. showed that oral gavage of female NOD mice with *Akkermensia muciniphila* from weaning until 10 weeks of age delayed diabetes (69). Using a chemically induced enhanced gut permeability condition, Sofi et al. showed that oral administration of heat-killed (HK) *B. fragilis* suppressed autoimmunity in NOD mice *(33).* On the other hand, intravenous injection of NOD mice with HK *B. fragilis* accelerated disease progression. Indeed, the importance of immunization route is well appreciated in vaccinology (70) and highlighted by our experiments where oral gavage of female NOD mice with *P. distasonis* stimulated a pathogenic response via the mucosal immune system whereas subcutaneous immunization with the *P. distasonis* insB:9-23 mimic stimulated protection. This latter finding corroborates a previous report demonstrating that immunization with the native insB:9-23 peptide reduces T1D incidence in female NOD mice (35).

To our knowledge, *P. distasonis* is the first bacterium that can accelerate the disease onset in the NOD mice. We showed that *P. distasonis* is not naturally present in the NOD mice gut microbiome in our SPF facility. Although this provides a good control to determine the effects of *P. distasonis* on T1D onset, it has limitations. Because *P. distasonis* is not previously used for genetic mutations and do not have established protocols, we failed to make a mutant of *P. distasonis* that has a deletion or mutations of the mimic peptide. Further *in vivo* studies are needed to establish the direct link between the mimic peptide and the effects of the colonization.

Today, we have databases with enormous amounts of microbial and microbiome sequencing data that can be levereaged to address the role of molecular mimicry in autoimmunity. Indeed, we see the return of the molecular mimicry hypothesis in the autoimmunity field with recent studies on T1D (66), lupus (71), inflammatory cardiomyopathy (72), and multiple sclerosis (73). These studies, including ours, constitute a new link to gut antigens and autoimmune diseases with the potential to ultimately provide new tools including vaccines, antibiotics or probiotics for

prevention and treatment of autoimmune disease. The uniqueness of the *P. distasonis* insB:9-23 mimic peptide in NCBI databases supports our ongoing efforts to characterize its effect based on Koch's postulates.

In conclusion, our data show that the *P. distasonis* insB:9-23 like peptide stimulates human and NOD mice T cells specific to native insB:9-23. Intestinal colonization of female NOD mice with *P. distasonis* accelerates autoimmune diabetes. This phenotype can be adoptively transferred to NOD.SCID mice demonstrating the direct role of immune cells stimulated by *P. distasonis.* More importantly, human data show that delayed exposure to the *P. distasonis* insB:9-23 mimic might be pathogenic in the first three years of life.

## MATERIAL AND METHODS

### Bioinformatics

We performed a comprehensive bioinformatics search for the presence of the microbial peptide sequences with homology to human insB:9-23 sequence at the National Center for Biotechnology Information (NCBI). A bioinformatics search was performed by NCBI BLASTp using insB:9-23 sequence as query against viral (NCBI taxonomic ID: 10239), bacterial (NCBI taxonomic ID: 2) and fungal (NCBI taxonomic ID: 10239) proteomes. The whole peptide sequence of each significant hit was compared with insB:9-23 using a multiple sequence alignment program (Clustal Omega) to determine the number of the identical and conserved residues. This yielded the data in Tables 1 and S1. An additional bioinformatics search was performed to determine whether P. distasonis peptide is unique. We used P. distasonis peptide (15 aa) or P. distasonis hypoxanthine phosphoribosyltransferase protein sequences as queries and searched against BLASTp using non redundant protein sequences. This yielded the data in Figure S1 and Supplementary documents 1-2.

### Mouse procedures

NOD/ShiLtJ (NOD) and NOD. Cg-*Pcrkdc scid*/J (NOD.Scid) mice were purchased from Jackson Laboratory. Mice were maintained and bred in Boston College Animal Care Facility. All of the mice were maintained under specific pathogen-free conditions in a 12-h dark/light cycle with autoclaved food, water and bedding. All experiments complied with regulations and ethics guidelines of the National Institute of Health and were approved by the IACUC of Boston College (no B2019-003, 2019-004).

## Human Plasma Samples

Peripheral blood was collected from living subjects following the provision of written informed consent (and assent in the case of minors) in accordance with IRB approved protocols (University of Florida IRB# 201400703) and the Declaration of Helsinki.

## Human T-Cell Clone Stimulation.

Twenty 15-mer peptides (**Table 1**) used in human and mouse T-cell stimulation experiments were chemically synthesized by Genscript (TFA removal, >85% purity). The peptides were dissolved in DMSO at 20 mg/mL (~12 mM). Human T-cell clone stimulation assays were performed as previously described (74). Briefly, insulin B: 11-23-specific T-cell clones were stimulated in 96-well round bottom plates with irrelevant, specific, or microbial mimotope peptides in the presence of irradiated DQ8-transdimer-transfected HEK293 cells as APCs. 50 µl of supernatants from cultures of T cell clones were collected after 48 h stimulation and added to each well of 96-well round bottom plates precoated with IFN-γ (clone MD-1) capturing antibodies (BioLegend). After overnight incubation, bound cytokines were detected by biotinylated anti-IFN-γ (clone 4s.B3) and quantified using a Victor2 D time resolved fluorometer (Perkin Elmer). Experiments were performed in the presence of 1 µg/ml of anti-CD28 antibodies. Unless otherwise stated, peptide concentrations were 2.5 µM.

## Binding Model for *P. distasonis* peptide

Coordinates for the insB:9-23 peptide bound to HLA-DQ8 were superimposed on I-Ag7 complexed to GAD peptide. The insB:9-23 was extracted and merged with I-Ag7, and energy minimized to model peptide binding in register 2. Side chains of the insB:9-23 peptide were mutated to accommodate the register 3 shift, followed by energy minimization. *P. distasonis*

peptide and insB:9-23 peptide sequences were aligned and the coordinates mutated to the *P. distasonis* peptide, and the resulting model of peptide complexed to I-Ag7 was energy minimized. The MHCI binding predictions were made on 11/30/2019 using the IEDB analysis resource Consensus tool (75) which combines predictions from ANN aka NetMHC (4.0) (76-78), SMM (79) and Comblib (80) .

**NOD mice T-cell stimulation and antigen presentation assay**

We performed the experiments as described previously (29). The peptides were ordered from Genscript (TFA removal, >85% purity) and dissolved in a base buffer consisting of 50mM NaCl, 10mM HEPES, pH6.8 with 200uM TCEP. Because *P. distasonis* peptide has a neutral charge, we included 5% DMSO to dissolve it (final DMSO concentration is less than 1%). The C3g7 cell line, which express an abundance of MHC-II I-Ag7, was used as APC and were treated with 1/2log dilutions of peptide (starting from 10uM). These cells were then cultured with the IIT-3 or 8F10 T cell hybridomas for 18 h. Culture supernatants were assayed for IL-2 by incubation with the CTLL-2 cell line. CTLL-2 cells are responsive to IL-2 and only actively divide in the presence of IL-2. We then determined the 3H uptake (CPM) to measure how many CTLL cells are proliferating using a scintillation counter.

**Immunization of the NOD mice**

The experiments were performed as described previously (81). Briefly, 13 week old male NOD mice (n=2 mice per group) were immunized in the footpad with the *P. distasonis* peptide or insulin B:9-23 peptide (10nmoles/mouse). After 7 days, the draining lymph nodes were removed and pooled for examination by ELISpot. In the ELISpot assay, node cells were recalled with the various peptides to elicit either an IL-2 or IFN-g response. Spots were analyzed by Immunospot 5.0 (C.T.L.)

## Reanalysis of the published metagenomics data

BABYDIET 16S sequencing data (36) (22 cases and 22 matched controls) were provided by Dr. David Endesfelder (Scientific Computing Research Unit, Helmholtz Zentrum München, Munich, Germany). To determine the abundance of the OTUs corresponding to each group, we calculated the normalized average number of *P. distasonis* OTUs (Figure 4A) for each group based on the collection time of the stool samples, e.g. 0-1, 1-2 and 2-3 years. Data is shown with median OTU number/group normalized to the means of each sample. We downloaded the DIABIMMUNE data with the help of Dr. Alex Kostic. Because the reads were not ideal for a peptide search, we first assembled the reads using SPAdes (11) and they are available at https://github.com/ablab/spades. We used these assembled contigs for a TBLASTN search to identify "RILVELLYLVCSEYL" encoding sequences in these samples. We then classified the data based on the collection time of the stool samples, e.g. 0-1, 1-2 and 2-3 years (Figure 4B) and country (Figure 4C).

## Bacterial culture

*Parabacteroides distasonis D 13* strain was purchased from Dr. Emma Allen-Vercoe's laboratory at University of Guelph. Dr. Allen-Vercoe's group isolated this bacterium from the colon of a ulcerative colitis patient. *P. distasonis D13* strain and *Bacteroides fragilis* (ATCC® 25285) were cultured in anaerobic culture broth (Tryptic Soy Broth supplemented with 5ug/ml Hemin (BD Biosciences) and 1ug/ml Vitamin K1 (VWR)) at 37°C in anaerobic chamber (Coy Laboratory Product).

## Oral gavage of *Parabacteroides distasonis* into NOD mice

After *P. distasonis* were cultured from frozen stock at 37°C overnight (OD=1.5), *P. distasonis* were collected by centrifuging at 4000 rpm for 10 min and washed 3 times with sterile saline

(Baxter). After the last wash, *P. distasonis* were re-suspended with saline and oral gavaged using 22ga plastic feeding tube (Instech Laboratories) (100ul/mouse, $10^9$ CFU/mouse). 3-week-old NOD mice were oral gavaged with *Parabacteroides distasonis D13* daily for four weeks right after weaning for 4 weeks (n=40/group/sex). Control groups were gavaged with sterile saline.

**Fecal bacterial DNA extraction**

Mouse fecal samples were collected as fecal pellets in Eppendorf tubes and stored at -80°C right after collection. The DNA were contracted from 100 mg mouse fecal samples using QIAamp PowerFecal Pro DNA kit (Qiagen) following manufacturer's instruction.

**Quantification of *Parabacteroides distasonis* by qPCR**

Bacterial DNA was extracted from NOD mice fecal samples (9-week old) 2 weeks after oral gavage was completed as described in Fecal bacteria DNA extraction section. qPCR was conducted using QuantStudio 3 Real-Time PCR System (Applied Biosystems) at 95°C for 10 mins followed by 40 cycles of 15 sec at 95°C and 1 min at 60°C with Power SYBR Green Master Mix (Applied Biosystems) following manufacturer's instruction. The primers were described previously and listed in Table S5 (82, 83). The relevant abundance of *Parabacteroides distasonis* was determined by normalized with *Eubacteria.*

**HPT expression in *Parabacteroides distasonis* by RT-qPCR**

Bacterial RNA was extracted from Parabacteroides distasonis using ZymoBIOMICS DNA/RNA kit (Zymo Research). RNA reverse-transcription and first strand synthesis were performed using QuantStudio 3 (Applied Biosystems) following manufacturer's instruction. cDNAs were applied for quantitative PCR through the same system mentioned above All sample reactions running in triplicate. The primers were designed to reverse transcribe 200 bp fragments of HPT using primer

blast. The primers target all bacteria 16S and *Parabacteroides distasonis* 16S rRNA were described previously and listed in Table S5(84). Data obtained were normalized using 16S rRNA expression levels as reference and relative expression was determined by calculating the ΔΔCq.

**Immunization of NOD mice with *P. distasonis* peptide**

The peptides were synthesized by GenScript USA Inc. 15-mer peptides, Insulin epitope peptide (LVELLYLVCSEYLNH), insulin 2 peptide (SHLVEALYLCGERG), or 14-mer tetanus toxin peptide (QYIKANSKFIGIFE) (Purity>85%; 10ug/mouse/week) in saline were subcutaneously injected into NOD mice (n=20) weekly from 4 weeks old until 25 weeks old as described previously (35). Tail vein blood glucose was monitored weekly and mice with >250mg/dl for two consecutive days as diabetic.

**Immune cells transplantation**

Splenocytes were isolated from spleen and pancreatic lymph nodes of 15 weeks donor NOD mice by filtering through a sterile nylon mesh followed by red blood cell lysis with ACK (Lonza). The isolated splenocytes were intravenously injected through lateral tail vein into recipient NOD SCID mice (9 weeks old) ($5x10^7$ cells/mouse). Donor NOD mice and recipient NOD.SCID mice were sex matched. Recipient mice were monitored for diabetes by checking tail vein blood glucose level (>250mg/dl) twice per week. The experiment terminated 11 weeks after the transplantation unless the mice were diagnosed with diabetes. Donor mice were 15-week male or female NOD mice colonized with either *P. distasonis* or their sex matched saline control (n=16).

**Insulitis score**

Pancreas were isolated from *P. distasonis* colonized 12 weeks NOD mice and control mice (n=5) followed by fixation with 4% paraformaldehyde overnight at 4°C, embedding with paraffin,

sectioning into 5µm thickness and stained with hematoxylin-eosin (Harvard University, BIDMC Histology Core). Slides were analyzed using EVOS XL Core microscope with a LPlan PH2 10×/0.25 and a LPlan PH2 20×/0.40 objective. The pancreatic insulitis was screened and evaluated as described previously (85).

**Western Blot analysis**

Bacteria lysis protein were extracted with CelLytic B Cell Lysis Reagent (Sigma) following manufacturer's instruction. Protein concentration were determined by BCA assay (Thermo Scientific). 20 µg bacterial protein was loaded for well for the gel. Standard western blots were performed by using tank blotting (Bio-rad) as membrane transfer equipment for 1h at 4°C. Membrane were then blocked with 5% non fat milk+PBST. After washing, each membrane was incubated with mouse serum (1: 2,500) or human serum (1: 10,000) overnight at 4°C followed by washing and Sheep anti-mouse (1:3000, Millipore) or goat anti-human antibody (1:3000, Santa Cruz) incubation for 1h. After washing, the blots were developed with chemiluminescent substrate ECL (Thermo Fisher)

**Endotoxin and IAA quantification and ELISA**

12-week NOD Mouse serum was collected and stored at −80 °C until use. Serum endotoxin level was measured by using a Pierce Chromogenic Endotoxin Quant Kit (Thermo Scientific) following the manufacturers' instructions. We used mouse IAA ELISA Kit (MyBioSource, MBS26087) to measure IAA levels. The experiment was completed according manufacturer's instructions.

**Luminex**

MCYTMAG-70K-PX32 Milliplex Mouse Cytokine/Chemokine MAGNETIC BEAD Premixed 32 Plex Kit (**MilliporeSigma)** was used to determine circulating cytokines and chemokines in

mice plasma. The experiment was performed according to manufacturer's instructions and the plates were read using Luminex® 200™ (Thermo Fisher) at Multiplex Core of Forsyth Institute.

**Statistics**

Data are presented as the mean ± SEM. Survival curves were analyzed by log-rank (Mantel-cox) test. Statistical significance was evaluated using unpaired two-tailed Student's *t*-test for two-group comparison or ANOVA, followed by a Tukey-Kramer post-hoc, Bonferroni's post-hoc where appropriate. A P value of less than 0.05 was considered significant (*).

**Proteomics Analysis.** Gel slices were submitted for mass-spectrometry analysis and protein identification, which were performed at the Taplin Mass Spectrometry Facility at Harvard Medical School as previously described (86)

## REFERENCES


1. Pugliese A. Autoreactive T cells in type 1 diabetes. *J Clin Invest.* 2017;127(8):2881-91.
2. Patterson CC, Harjutsalo V, Rosenbauer J, Neu A, Cinek O, Skrivarhaug T, et al. Trends and cyclical variation in the incidence of childhood type 1 diabetes in 26 European centres in the 25 year period 1989-2013: a multicentre prospective registration study. *Diabetologia.* 2019;62(3):408-17.
3. Mayer-Davis EJ, Lawrence JM, Dabelea D, Divers J, Isom S, Dolan L, et al. Incidence Trends of Type 1 and Type 2 Diabetes among Youths, 2002-2012. *N Engl J Med.* 2017;376(15):1419-29.
4. Kondrashova A, Reunanen A, Romanov A, Karvonen A, Viskari H, Vesikari T, et al. A six-fold gradient in the incidence of type 1 diabetes at the eastern border of Finland. *Ann Med.* 2005;37(1):67-72.
5. Redondo MJ, Jeffrey J, Fain PR, Eisenbarth GS, and Orban T. Concordance for islet autoimmunity among monozygotic twins. *N Engl J Med.* 2008;359(26):2849-50.
6. Zhao G, Vatanen T, Droit L, Park A, Kostic AD, Poon TW, et al. Intestinal virome changes precede autoimmunity in type I diabetes-susceptible children. *Proc Natl Acad Sci U S A.* 2017;114(30):E6166-E75.
7. Op de Beeck A, and Eizirik DL. Viral infections in type 1 diabetes mellitus--why the beta cells? *Nat Rev Endocrinol.* 2016;12(5):263-73.
8. Christen U, Hintermann E, Holdener M, and von Herrath MG. Viral triggers for autoimmunity: is the 'glass of molecular mimicry' half full or half empty? *J Autoimmun.* 2010;34(1):38-44.
9. Rewers M, and Ludvigsson J. Environmental risk factors for type 1 diabetes. *Lancet.* 2016;387(10035):2340-8.
10. Davis-Richardson AG, Ardissone AN, Dias R, Simell V, Leonard MT, Kemppainen KM, et al. Bacteroides dorei dominates gut microbiome prior to autoimmunity in Finnish children at high risk for type 1 diabetes. *Frontiers in microbiology.* 2014;5:678.
11. Vatanen T, Franzosa EA, Schwager R, Tripathi S, Arthur TD, Vehik K, et al. The human gut microbiome in early-onset type 1 diabetes from the TEDDY study. *Nature.* 2018;562(7728):589-94.

12. Kostic AD, Gevers D, Siljander H, Vatanen T, Hyotylainen T, Hamalainen AM, et al. The dynamics of the human infant gut microbiome in development and in progression toward type 1 diabetes. *Cell Host Microbe.* 2015;17(2):260-73.
13. Vatanen T, Kostic AD, d'Hennezel E, Siljander H, Franzosa EA, Yassour M, et al. Variation in Microbiome LPS Immunogenicity Contributes to Autoimmunity in Humans. *Cell.* 2016;165(4):842-53.
14. Dedrick S, Sundaresh B, Huang Q, Brady C, Yoo T, Cronin C, et al. The Role of Gut Microbiota and Environmental Factors in Type 1 Diabetes Pathogenesis. *Front Endocrinol (Lausanne).* 2020;11:78.
15. Coppieters KT, Boettler T, and von Herrath M. Virus infections in type 1 diabetes. *Cold Spring Harb Perspect Med.* 2012;2(1):a007682.
16. Atkinson MA, Eisenbarth GS, and Michels AW. Type 1 diabetes. *Lancet.* 2014;383(9911):69-82.
17. Peters L, Posgai A, and Brusko TM. Islet-immune interactions in type 1 diabetes: the nexus of beta cell destruction. *Clin Exp Immunol.* 2019;198(3):326-40.
18. Zhang L, Nakayama M, and Eisenbarth GS. Insulin as an autoantigen in NOD/human diabetes. *Curr Opin Immunol.* 2008;20(1):111-8.
19. Alleva DG, Crowe PD, Jin L, Kwok WW, Ling N, Gottschalk M, et al. A disease-associated cellular immune response in type 1 diabetics to an immunodominant epitope of insulin. *J Clin Invest.* 2001;107(2):173-80.
20. Palmer JP, Asplin CM, Clemons P, Lyen K, Tatpati O, Raghu PK, et al. Insulin antibodies in insulin-dependent diabetics before insulin treatment. *Science.* 1983;222(4630):1337-9.
21. Steck AK, Johnson K, Barriga KJ, Miao D, Yu L, Hutton JC, et al. Age of islet autoantibody appearance and mean levels of insulin, but not GAD or IA-2 autoantibodies, predict age of diagnosis of type 1 diabetes: diabetes autoimmunity study in the young. *Diabetes Care.* 2011;34(6):1397-9.
22. Unanue ER. Antigen presentation in the autoimmune diabetes of the NOD mouse. *Annu Rev Immunol.* 2014;32:579-608.
23. Daniel D, Gill RG, Schloot N, and Wegmann D. Epitope specificity, cytokine production profile and diabetogenic activity of insulin-specific T cell clones isolated from NOD mice. *Eur J Immunol.* 1995;25(4):1056-62.

585 24. Pathiraja V, Kuehlich JP, Campbell PD, Krishnamurthy B, Loudovaris T, Coates PT, et al.
586 Proinsulin-specific, HLA-DQ8, and HLA-DQ8-transdimer-restricted CD4+ T cells
587 infiltrate islets in type 1 diabetes. *Diabetes.* 2015;64(1):172-82.
588 25. Michels AW, Landry LG, McDaniel KA, Yu L, Campbell-Thompson M, Kwok WW, et
589 al. Islet-Derived CD4 T Cells Targeting Proinsulin in Human Autoimmune Diabetes.
590 *Diabetes.* 2017;66(3):722-34.
591 26. Nakayama M, McDaniel K, Fitzgerald-Miller L, Kiekhaefer C, Snell-Bergeon JK,
592 Davidson HW, et al. Regulatory vs. inflammatory cytokine T-cell responses to mutated
593 insulin peptides in healthy and type 1 diabetic subjects. *Proc Natl Acad Sci U S A.*
594 2015;112(14):4429-34.
595 27. Yang J, Chow IT, Sosinowski T, Torres-Chinn N, Greenbaum CJ, James EA, et al.
596 Autoreactive T cells specific for insulin B:11-23 recognize a low-affinity peptide register
597 in human subjects with autoimmune diabetes. *Proc Natl Acad Sci U S A.*
598 2014;111(41):14840-5.
599 28. Cusick MF, Libbey JE, and Fujinami RS. Molecular mimicry as a mechanism of
600 autoimmune disease. *Clin Rev Allergy Immunol.* 2012;42(1):102-11.
601 29. Wan X, Zinselmeyer BH, Zakharov PN, Vomund AN, Taniguchi R, Santambrogio L, et
602 al. Pancreatic islets communicate with lymphoid tissues via exocytosis of insulin peptides.
603 *Nature.* 2018;560(7716):107-11.
604 30. Sakamoto M, and Benno Y. Reclassification of Bacteroides distasonis, Bacteroides
605 goldsteinii and Bacteroides merdae as Parabacteroides distasonis gen. nov., comb. nov.,
606 Parabacteroides goldsteinii comb. nov. and Parabacteroides merdae comb. nov. *Int J Syst*
607 *Evol Microbiol.* 2006;56(Pt 7):1599-605.
608 31. Abuaita BH, and Withey JH. Bicarbonate Induces Vibrio cholerae virulence gene
609 expression by enhancing ToxT activity. *Infect Immun.* 2009;77(9):4111-20.
610 32. Stadinski BD, Zhang L, Crawford F, Marrack P, Eisenbarth GS, and Kappler JW.
611 Diabetogenic T cells recognize insulin bound to IAg7 in an unexpected, weakly binding
612 register. *Proc Natl Acad Sci U S A.* 2010;107(24):10978-83.
613 33. Sofi MH, Johnson BM, Gudi RR, Jolly A, Gaudreau MC, and Vasu C. Polysaccharide A-
614 Dependent Opposing Effects of Mucosal and Systemic Exposures to Human Gut
615 Commensal Bacteroides fragilis in Type 1 Diabetes. *Diabetes.* 2019;68(10):1975-89.

34. Fuchtenbusch M, Larger E, Thebault K, and Boitard C. Transfer of diabetes from prediabetic NOD mice to NOD-SCID/SCID mice: association with pancreatic insulin content. *Horm Metab Res.* 2005;37(2):63-7.

35. Devendra D, Paronen J, Moriyama H, Miao D, Eisenbarth GS, and Liu E. Differential immune response to B:9-23 insulin 1 and insulin 2 peptides in animal models of type 1 diabetes. *J Autoimmun.* 2004;23(1):17-26.

36. Endesfelder D, zu Castell W, Ardissone A, Davis-Richardson AG, Achenbach P, Hagen M, et al. Compromised gut microbiota networks in children with anti-islet cell autoimmunity. *Diabetes.* 2014;63(6):2006-14.

37. Mason D. A very high level of crossreactivity is an essential feature of the T-cell receptor. *Immunol Today.* 1998;19(9):395-404.

38. Calis JJ, de Boer RJ, and Kesmir C. Degenerate T-cell recognition of peptides on MHC molecules creates large holes in the T-cell repertoire. *PLoS Comput Biol.* 2012;8(3):e1002412.

39. Wucherpfennig KW, and Strominger JL. Molecular mimicry in T cell-mediated autoimmunity: viral peptides activate human T cell clones specific for myelin basic protein. *Cell.* 1995;80(5):695-705.

40. Mana P, Goodyear M, Bernard C, Tomioka R, Freire-Garabal M, and Linares D. Tolerance induction by molecular mimicry: prevention and suppression of experimental autoimmune encephalomyelitis with the milk protein butyrophilin. *Int Immunol.* 2004;16(3):489-99.

41. Atkinson MA, Bowman MA, Campbell L, Darrow BL, Kaufman DL, and Maclaren NK. Cellular immunity to a determinant common to glutamate decarboxylase and coxsackie virus in insulin-dependent diabetes. *J Clin Invest.* 1994;94(5):2125-9.

42. Schloot NC, Willemen SJ, Duinkerken G, Drijfhout JW, de Vries RR, and Roep BO. Molecular mimicry in type 1 diabetes mellitus revisited: T-cell clones to GAD65 peptides with sequence homology to Coxsackie or proinsulin peptides do not crossreact with homologous counterpart. *Hum Immunol.* 2001;62(4):299-309.

43. Tian J, Lehmann PV, and Kaufman DL. T cell cross-reactivity between coxsackievirus and glutamate decarboxylase is associated with a murine diabetes susceptibility allele. *J Exp Med.* 1994;180(5):1979-84.

646 44. Honeyman MC, Stone NL, Falk BA, Nepom G, and Harrison LC. Evidence for molecular
647 mimicry between human T cell epitopes in rotavirus and pancreatic islet autoantigens. *J*
648 *Immunol.* 2010;184(4):2204-10.
649 45. Maruvada P, Leone V, Kaplan LM, and Chang EB. The Human Microbiome and Obesity:
650 Moving beyond Associations. *Cell Host Microbe.* 2017;22(5):589-99.
651 46. Rinaldi M, Perricone R, Blank M, Perricone C, and Shoenfeld Y. Anti-Saccharomyces
652 cerevisiae autoantibodies in autoimmune diseases: from bread baking to autoimmunity.
653 *Clin Rev Allergy Immunol.* 2013;45(2):152-61.
654 47. Gevers D, Kugathasan S, Denson LA, Vazquez-Baeza Y, Van Treuren W, Ren B, et al.
655 The treatment-naive microbiome in new-onset Crohn's disease. *Cell Host Microbe.*
656 2014;15(3):382-92.
657 48. Lamps LW, Madhusudhan KT, Havens JM, Greenson JK, Bronner MP, Chiles MC, et al.
658 Pathogenic Yersinia DNA is detected in bowel and mesenteric lymph nodes from patients
659 with Crohn's disease. *The American journal of surgical pathology.* 2003;27(2):220-7.
660 49. Chassaing B, Rolhion N, de Vallee A, Salim SY, Prorok-Hamon M, Neut C, et al. Crohn
661 disease--associated adherent-invasive E. coli bacteria target mouse and human Peyer's
662 patches via long polar fimbriae. *J Clin Invest.* 2011;121(3):966-75.
663 50. Carding S, Verbeke K, Vipond DT, Corfe BM, and Owen LJ. Dysbiosis of the gut
664 microbiota in disease. *Microb Ecol Health Dis.* 2015;26:26191.
665 51. Frank DN, St Amand AL, Feldman RA, Boedeker EC, Harpaz N, and Pace NR. Molecular-
666 phylogenetic characterization of microbial community imbalances in human inflammatory
667 bowel diseases. *Proc Natl Acad Sci U S A.* 2007;104(34):13780-5.
668 52. Navaneethan U, Venkatesh PG, and Shen B. Clostridium difficile infection and
669 inflammatory bowel disease: understanding the evolving relationship. *World J*
670 *Gastroenterol.* 2010;16(39):4892-904.
671 53. Quagliariello A, Aloisio I, Bozzi Cionci N, Luiselli D, D'Auria G, Martinez-Priego L, et
672 al. Effect of Bifidobacterium breve on the Intestinal Microbiota of Coeliac Children on a
673 Gluten Free Diet: A Pilot Study. *Nutrients.* 2016;8(10).
674 54. Heintz-Buschart A, May P, Laczny CC, Lebrun LA, Bellora C, Krishna A, et al. Integrated
675 multi-omics of the human gut microbiome in a case study of familial type 1 diabetes. *Nat*
676 *Microbiol.* 2016;2:16180.

677 55. Stewart CJ, Ajami NJ, O'Brien JL, Hutchinson DS, Smith DP, Wong MC, et al. Temporal
678 development of the gut microbiome in early childhood from the TEDDY study. *Nature.*
679 2018;562(7728):583-8.
680 56. Lathrop SK, Bloom SM, Rao SM, Nutsch K, Lio CW, Santacruz N, et al. Peripheral
681 education of the immune system by colonic commensal microbiota. *Nature.*
682 2011;478(7368):250-4.
683 57. Nakayama M, Abiru N, Moriyama H, Babaya N, Liu E, Miao D, et al. Prime role for an
684 insulin epitope in the development of type 1 diabetes in NOD mice. *Nature.*
685 2005;435(7039):220-3.
686 58. Higashide T, Kawamura T, Nagata M, Kotani R, Kimura K, Hirose M, et al. T cell epitope
687 mapping study with insulin overlapping peptides using ELISPOT assay in Japanese
688 children and adolescents with type 1 diabetes. *Pediatr Res.* 2006;59(3):445-50.
689 59. Kent SC, Chen Y, Bregoli L, Clemmings SM, Kenyon NS, Ricordi C, et al. Expanded T
690 cells from pancreatic lymph nodes of type 1 diabetic subjects recognize an insulin epitope.
691 *Nature.* 2005;435(7039):224-8.
692 60. Mannering SI, Harrison LC, Williamson NA, Morris JS, Thearle DJ, Jensen KP, et al. The
693 insulin A-chain epitope recognized by human T cells is posttranslationally modified. *J Exp*
694 *Med.* 2005;202(9):1191-7.
695 61. Mannering SI, Di Carluccio AR, and Elso CM. Neoepitopes: a new take on beta cell
696 autoimmunity in type 1 diabetes. *Diabetologia.* 2019;62(3):351-6.
697 62. Purcell AW, Sechi S, and DiLorenzo TP. The Evolving Landscape of Autoantigen
698 Discovery and Characterization in Type 1 Diabetes. *Diabetes.* 2019;68(5):879-86.
699 63. Delong T, Wiles TA, Baker RL, Bradley B, Barbour G, Reisdorph R, et al. Pathogenic
700 CD4 T cells in type 1 diabetes recognize epitopes formed by peptide fusion. *Science.*
701 2016;351(6274):711-4.
702 64. Kracht MJ, van Lummel M, Nikolic T, Joosten AM, Laban S, van der Slik AR, et al.
703 Autoimmunity against a defective ribosomal insulin gene product in type 1 diabetes. *Nat*
704 *Med.* 2017;23(4):501-7.
705 65. Babon JA, DeNicola ME, Blodgett DM, Crevecoeur I, Buttrick TS, Maehr R, et al.
706 Analysis of self-antigen specificity of islet-infiltrating T cells from human donors with type
707 1 diabetes. *Nat Med.* 2016;22(12):1482-7.

66. Tai N, Peng J, Liu F, Gulden E, Hu Y, Zhang X, et al. Microbial antigen mimics activate diabetogenic CD8 T cells in NOD mice. *J Exp Med.* 2016;213(10):2129-46.

67. Markle JG, Frank DN, Mortin-Toth S, Robertson CE, Feazel LM, Rolle-Kampczyk U, et al. Sex differences in the gut microbiome drive hormone-dependent regulation of autoimmunity. *Science.* 2013;339(6123):1084-8.

68. Kriegel MA, Sefik E, Hill JA, Wu HJ, Benoist C, and Mathis D. Naturally transmitted segmented filamentous bacteria segregate with diabetes protection in nonobese diabetic mice. *Proc Natl Acad Sci U S A.* 2011;108(28):11548-53.

69. Hanninen A, Toivonen R, Poysti S, Belzer C, Plovier H, Ouwerkerk JP, et al. Akkermansia muciniphila induces gut microbiota remodelling and controls islet autoimmunity in NOD mice. *Gut.* 2018;67(8):1445-53.

70. Song L, Xiong D, Song H, Wu L, Zhang M, Kang X, et al. Mucosal and Systemic Immune Responses to Influenza H7N9 Antigen HA1-2 Co-Delivered Intranasally with Flagellin or Polyethyleneimine in Mice and Chickens. *Front Immunol.* 2017;8:326.

71. Greiling TM, Dehner C, Chen X, Hughes K, Iniguez AJ, Boccitto M, et al. Commensal orthologs of the human autoantigen Ro60 as triggers of autoimmunity in lupus. *Sci Transl Med.* 2018;10(434).

72. Gil-Cruz C, Perez-Shibayama C, De Martin A, Ronchi F, van der Borght K, Niederer R, et al. Microbiota-derived peptide mimics drive lethal inflammatory cardiomyopathy. *Science.* 2019;366(6467):881-6.

73. Harkiolaki M, Holmes SL, Svendsen P, Gregersen JW, Jensen LT, McMahon R, et al. T cell-mediated autoimmune disease due to low-affinity crossreactivity to common microbial peptides. *Immunity.* 2009;30(3):348-57.

74. Chow IT, Gates TJ, Papadopoulos GK, Moustakas AK, Kolawole EM, Notturno RJ, et al. Discriminative T cell recognition of cross-reactive islet-antigens is associated with HLA-DQ8 transdimer-mediated autoimmune diabetes. *Sci Adv.* 2019;5(8):eaaw9336.

75. Kim Y, Ponomarenko J, Zhu Z, Tamang D, Wang P, Greenbaum J, et al. Immune epitope database analysis resource. *Nucleic Acids Res.* 2012;40(Web Server issue):W525-30.

76. Nielsen M, Lundegaard C, Worning P, Lauemoller SL, Lamberth K, Buus S, et al. Reliable prediction of T-cell epitopes using neural networks with novel sequence representations. *Protein Sci.* 2003;12(5):1007-17.

77. Lundegaard C, Lamberth K, Harndahl M, Buus S, Lund O, and Nielsen M. NetMHC-3.0: accurate web accessible predictions of human, mouse and monkey MHC class I affinities for peptides of length 8-11. *Nucleic Acids Res.* 2008;36(Web Server issue):W509-12.

78. Andreatta M, and Nielsen M. Gapped sequence alignment using artificial neural networks: application to the MHC class I system. *Bioinformatics.* 2016;32(4):511-7.

79. Peters B, and Sette A. Generating quantitative models describing the sequence specificity of biological processes with the stabilized matrix method. *BMC Bioinformatics.* 2005;6:132.

80. Sidney J, Assarsson E, Moore C, Ngo S, Pinilla C, Sette A, et al. Quantitative peptide binding motifs for 19 human and mouse MHC class I molecules derived using positional scanning combinatorial peptide libraries. *Immunome Res.* 2008;4:2.

81. Mohan JF, Levisetti MG, Calderon B, Herzog JW, Petzold SJ, and Unanue ER. Unique autoreactive T cells recognize insulin peptides generated within the islets of Langerhans in autoimmune diabetes. *Nat Immunol.* 2010;11(4):350-4.

82. Dziarski R, Park SY, Kashyap DR, Dowd SE, and Gupta D. Pglyrp-Regulated Gut Microflora Prevotella falsenii, Parabacteroides distasonis and Bacteroides eggerthii Enhance and Alistipes finegoldii Attenuates Colitis in Mice. *PLoS One.* 2016;11(1):e0146162.

83. Croswell A, Amir E, Teggatz P, Barman M, and Salzman NH. Prolonged impact of antibiotics on intestinal microbial ecology and susceptibility to enteric Salmonella infection. *Infect Immun.* 2009;77(7):2741-53.

84. Srivastava S, Singh V, Kumar V, Verma PC, Srivastava R, Basu V, et al. Identification of regulatory elements in 16S rRNA gene of Acinetobacter species isolated from water sample. *Bioinformation.* 2008;3(4):173-6.

85. Flodstrom-Tullberg M, Yadav D, Hagerkvist R, Tsai D, Secrest P, Stotland A, et al. Target cell expression of suppressor of cytokine signaling-1 prevents diabetes in the NOD mouse. *Diabetes.* 2003;52(11):2696-700.

86. Pollock N, Dhiman R, Daifalla N, Farhat M, and Campos-Neto A. Discovery of a unique Mycobacterium tuberculosis protein through proteomic analysis of urine from patients with active tuberculosis. *Microbes Infect.* 2018;20(4):228-35.

## Acknowledgements

We first want to thank Prof. Emil Unanue and Dr. Anthony Vomund (University of Washington, St. Louis) for testing microbial insulins on T cell hybridomas, immunization experiments and with their help to interpret the data. Thanks to Jonathan.Dreyfuss and Hui Pan (Joslin Bioinformatics Core) for bioinformatics analysis. Thanks to Babak Momeni (Boston College) for sharing his laboratory's anaerobic chamber. We acknowledge BC Biology Department undergraduate students Tu Tran, Ruixu Huang with the microscopy work and David Kim and Scott Hsu for their help with the animal experiments. We thank to Alex Kostic, Tao Xu, Thomas Serwold and Shio Kobayashi (Joslin Diabetes Center) for the useful Discussion. Thanks to Annette Ziegler and David Endesfelder for providing the BABYDIET 16S sequencing data for reanalysis. Thanks to Amanda Posgai for editing the manuscript.

**Funding:** This work was supported by National Institutes of Health Grants 1K01DK117967-01 (to E.A.) and R01DK031026 and R01DK033201 (to C.R.K.) and NIH P01 AI042288 to MAA. E.A. was supported by The G. Harold and Leila Y. Mathers Charitable Foundation Research Grant and an Iacocca Family Foundation Fellowship.

**Author contributions:** Q.H assisted with all NOD mice experiments including peptide immunization, oral gavage, splenocyte transfer and ELISA/Luminex experiments, qPCR and Western blot analysis using human and mice plasma. A.V and E.U assisted with the experiments using NOD mice T-cell hybridomas. I.C and W.K assisted with the experiments using NOD mice T-cell clones. C.B and A.R assisted with the peptide immunization and oral gavage experiments. D.O and D.L assisted with MHC-binding models. M.A provided the human plasma samples. E.A

791 completed bioinformatics analysis. E.A and C.R.K designed the research. All authors assisted with
792 the analysis of the data. E.A supervised the project and wrote the paper.

793 **Competing Interests:** The authors do not have any conflict of interest related to this study.

794 **Data and materials availability:** Because the reads were not ideal for a peptide search, we first
795 assembled the reads using SPAdes (11) and they are available at https://github.com/ablab/spades.

# FIGURES

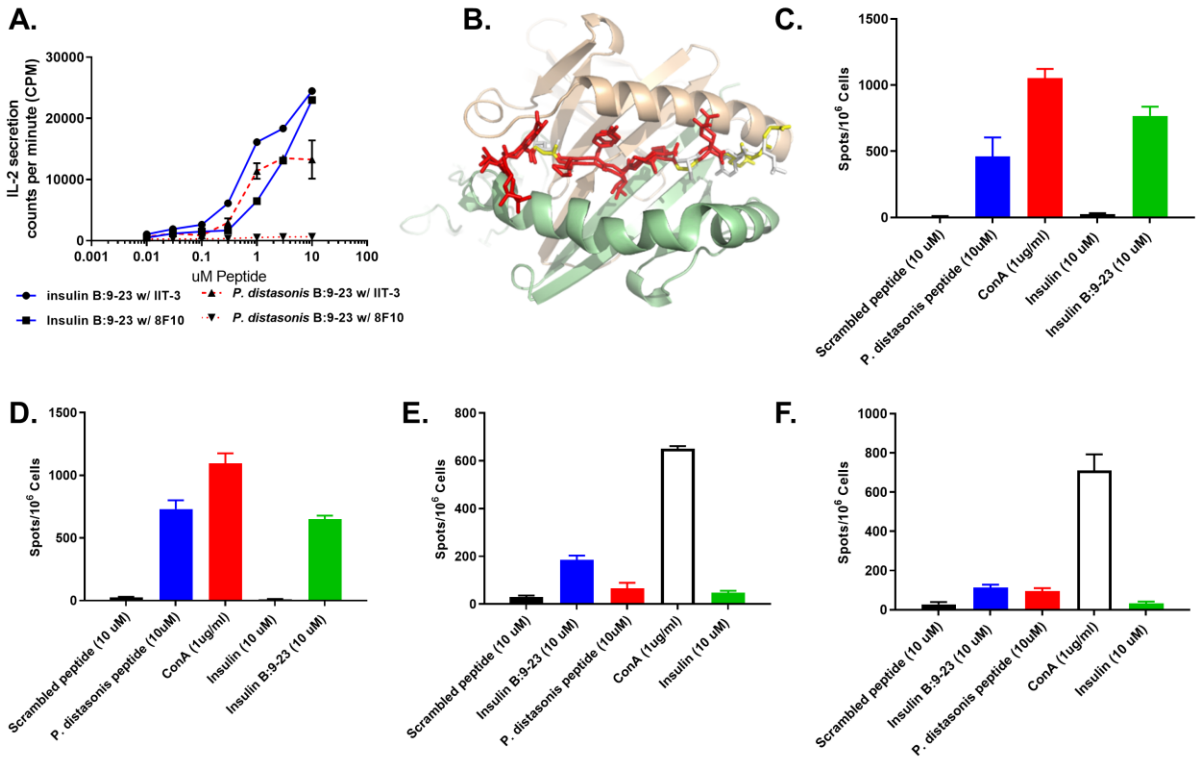


**Figure 1. *P. distasonis* insB:9-23peptide can stimulate insB:13-21 specific NOD mice T cell hybridomas and structurally mimic the epitope. (A)** CD4+ T cells recognize *P. distasonis* peptide. Response of the B:13–21-specific IIT-3 hybridomas (red) and B:12–20-specific8F10 (blue) to insulin B9-23 or *P. distasonis* peptides covalently linked to I-$A^{g7}$ expressed on macrophages. **(B)** Binding model for *P. distasonis* mimic peptide compared to insB9-23. In 3B, I-$A^{g7}$ α-chain in tan, I-$A^{g7}$ β-chain in green. insB:9-23 peptide shown as yellow sticks, *P. distasonis* peptide shown as white sticks. Red sticks and spheres show positions identical in *P. distasonis* peptide and insB:9-23 peptide. **(C-F)** Mice (n=2/group) were immunized with either insB:9-23 peptide (**C-E**) or *P. distasonis* peptide (**D-F**) and draining lymph nodes were removed and pooled after 7 days. Cells were stimulated either by *P. distasonis* peptide, insB:9-23, insulin, ConA (positive control) or scrambled peptide (negative control). Secretion of IL-2 (**C-D**) and interferon gamma (**E-F**) were determined by EliSPOT.

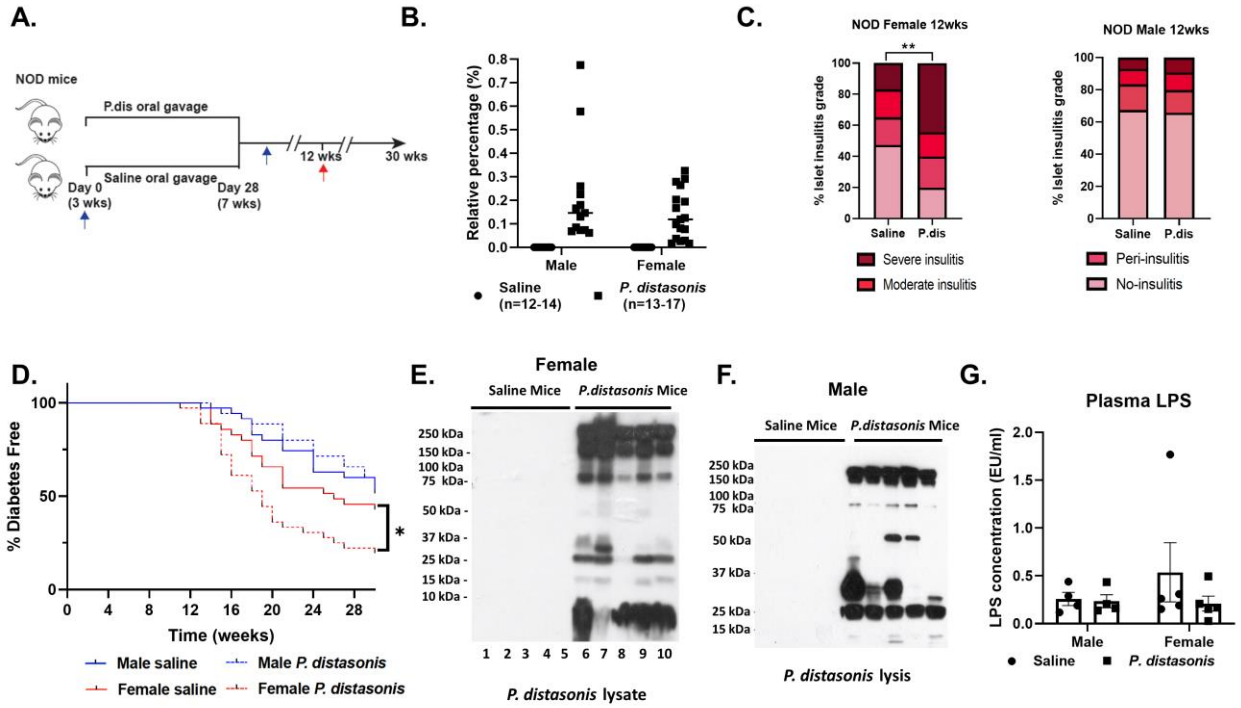


811

812 **Figure 2. P. distasonis colonization enhances disease onset in female NOD mice. (A)**
813 Schematic overview of the *P. distasonis* oral gavage experiments (n=40/group/sex). Blue arrow
814 shows fecal sample collection for qPCR experiments and red arrow shows when 5 mice were
815 removed from each group (week 12). **(B)** Relative abundance of *P. distasonis* in fecal samples
816 determined by qPCR (week 12, n=12-14/male, n=13-17/female). **(C)** Insulitis scores obtained from
817 mice at week 12 (n=5/group/sex). **(D)** Diabetes incidence in NOD mice (n=35/group/sex) after
818 daily saline or *P. distasonis* oral gavage for 30 days after weaning *(P<0.05)*. **(E-F)** Western blot
819 analysis using plasma samples from (E) female and (F) male mice either oral gavaged with *P.*
820 *distasonis* or saline (week 12, n=5/group/sex). **(G)** Plasma LPS levels (week 12, n=5/group/sex).

821

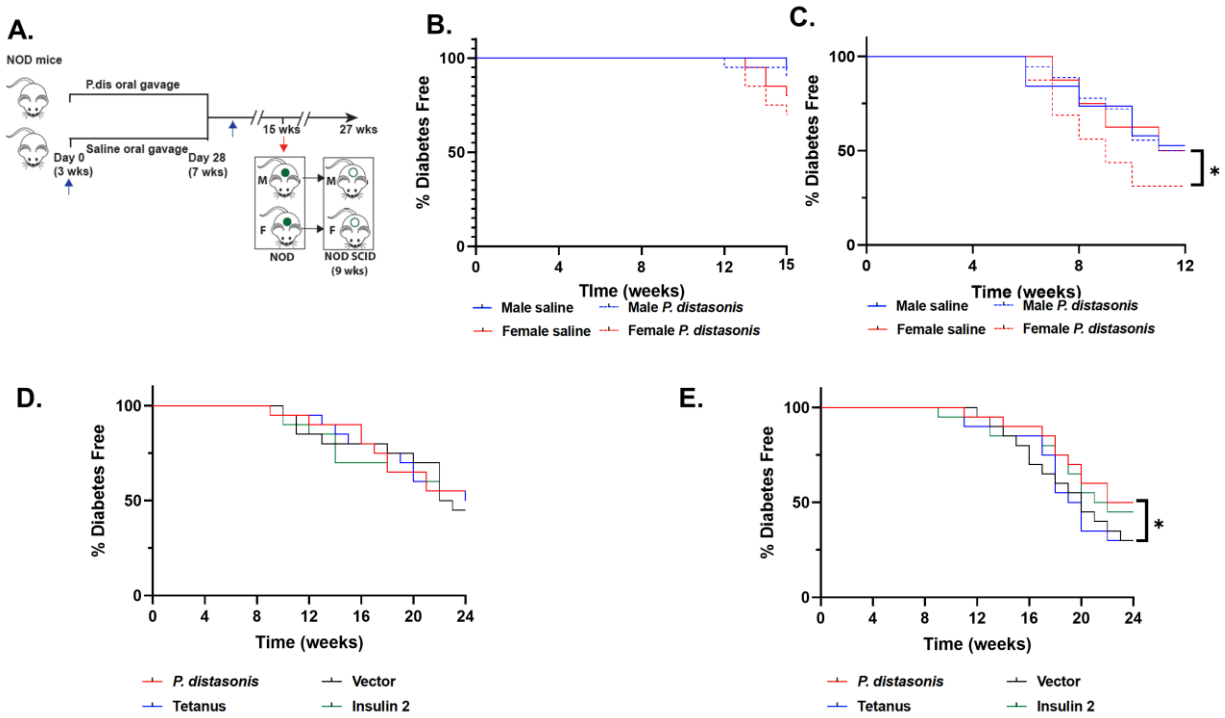


822

823 **Figure 3. Adoptive transfer accelerated diabetes in female NOD.SCID mice. (A)** Schematic
824 overview of the adoptive transfer experiments from NOD mice to NOD.SCID mice. $5x10^7$
825 splenocytes/mouse were transferred from individual NOD mice to NOD.SCID mice at 6 weeks of
826 age (1:1 ratio, same gender, n=16-20). **(B)** Diabetes incidence of donor NOD mice until adoptive
827 transfer (n=20). **(C)** Diabetes incidence of the recipient NOD.SCID mice after adoptive transfer
828 (n=16-20) *(P<0.05)*. **(D-E)** Diabetes incidence of (D) male and (E) female mice (n=20/group/sex)
829 immunized with either *P. distasonis* peptide or ins2:B:9-23 peptide or Tetanus toxin peptide or
830 vector *(P<0.05)*. Data are mean ± SEM. Survival curves were analyzed by log-rank (Mantel-cox)
831 test.

832

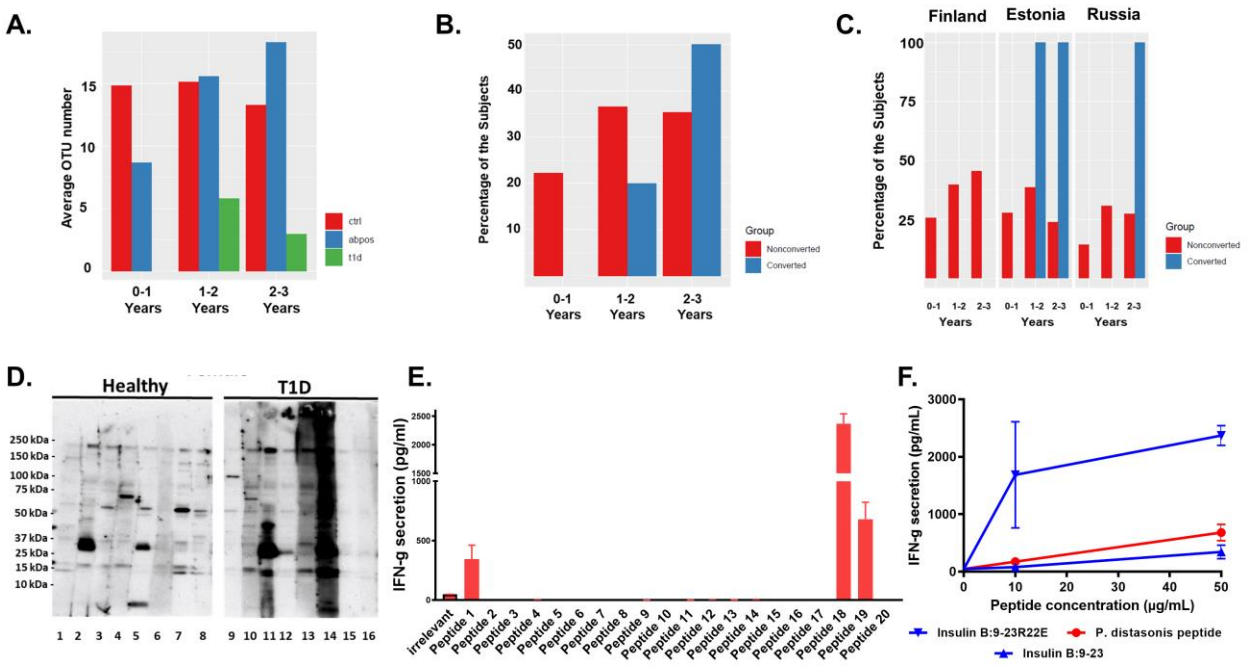


833

834 **Figure 4. Reanalysis of BABYDIET and DIABIMMUNE metagenome data for P. distasonis**
835 **peptide and identification of *P. distasonis* specific immune response in humans. (A)**
836 BABYDIET data was analyzed for the presence of *P. distasonis* OTUs in three different groups,
837 control, antibody-positive and T1D. **(B-C)** Reanalysis of DIABIMMUNE metagenome data for
838 the presence of *P. distasonis* ins9:23 like peptide **(B)** in all three countries and **(C)** in individual
839 countries. **(D)** Insulin B: 11-23-specific human T-cell clones were stimulated with each of selected
840 17 microbial peptides or 2 negative control (irrelevant and 20) peptides or 2 positive control (18-
841 19) (peptide concentration, 2.5 µM) and IFN-γ secretion was measured *(P<0.05)*. The
842 corresponding peptides for the numbers are listed in Table 1. **(E)** P. distasonis peptide produced a
843 dose response in stimulating IFN-γ secretion. B:9-23 and B:9-23R22E are positive controls of the
844 experiment. **(F)** Western blot analysis using plasma samples obtained from eight female subjects
845 with T1D or eight healthy female subjects against *P. distasonis* lysate. Data are mean ± SEM.
846 Survival curves were analyzed by log-rank (Mantel-cox) test.

847

848 **Table 1. The sequences of the microbial mimics of the insB:9-23 tested in this study. Red**

849 **indicate identical residues.**

| No | Classification | Source | B:9-23 like peptides | Identity |
|---|---|---|---|---|
| 1 | **Positive Control** | Human insulin B:9-23 peptide | **SHLVEALYLVCGERG** | Control |
| 2 | | Hyperactive peptide | **SHLVEALYLVCGEEG** | Control |
| 3 | **Human Gut Microbiome** | *Parabacteroides distasonis 33B* | **RILVELLYLVCSEYL** | 9 of 15 |
| 4 | | *Bacteroides sp. CAG:144* | **LDFKEALYLGCGDRT** | 8 of 15 |
| 5 | | *Ruminococcus gnavus CAG:126* | **DPRRSALYLFCGKRC** | 7 of 15 |
| 6 | | *Coprococcus eutactus* | **NHDKEALYIYCDETE** | 7 of 15 |
| 7 | | *Clostridiales bacterium VE202-14* | **VRAGYALFLVCDEEK** | 7 of 15 |
| 8 | **Human Genital Microbiome** | *Corynebacterium genitalium* | **FVHEDALHLVCGERI** | 9 of 15 |
| 9 | | *Lactobacillus vaginalis* | **LQSMEIPYLVCGERE** | 8 of 15 |
| 10 | **Viruses** | *Lymphocystis disease virus 1* | **AHLVAALQRVCGNRG** | 10 of 15 |
| 11 | | *Cyprinid herpesvirus 1* | **SHPNVFIALVCGERG** | 9 of 15 |
| 12 | | *Grouper iridovirus* | **GELIDALTEHCGDRG** | 7 of 15 |
| 13 | **Human pathogen** | *Burkholderia multivorans* | **LHLARALYEMCGEFP** | 8 of 15 |
| 14 | **Other microbes** | *Bradyrhizobium japonicum SEMIA 5079* | **VSGKHALYLYCGERG** | 9 of 15 |
| 15 | | *Streptomyces griseus* | **RDRVEALRLVCGEAM** | 9 of 15 |
| 16 | | *Tetrasphaera japonica T1-X7* | **HWLVEIAYLVCGDRR** | 8 of 15 |
| 17 | | *Saccharomonospora halophila* | **TAHGVAEYLVCGERR** | 8 of 15 |
| 18 | | *Brevundimonas sp. BAL3* | **WVGFETLYLYCGERL** | 8 of 15 |
| 19 | | *Metarhizium robertsii* | **DHWDEAGFLVCGERG** | 10 of 15 |
| 20 | **Negative Control** | *Negative control peptide (random)* | **LELYARVGVSECHGL** | Control |

850

851

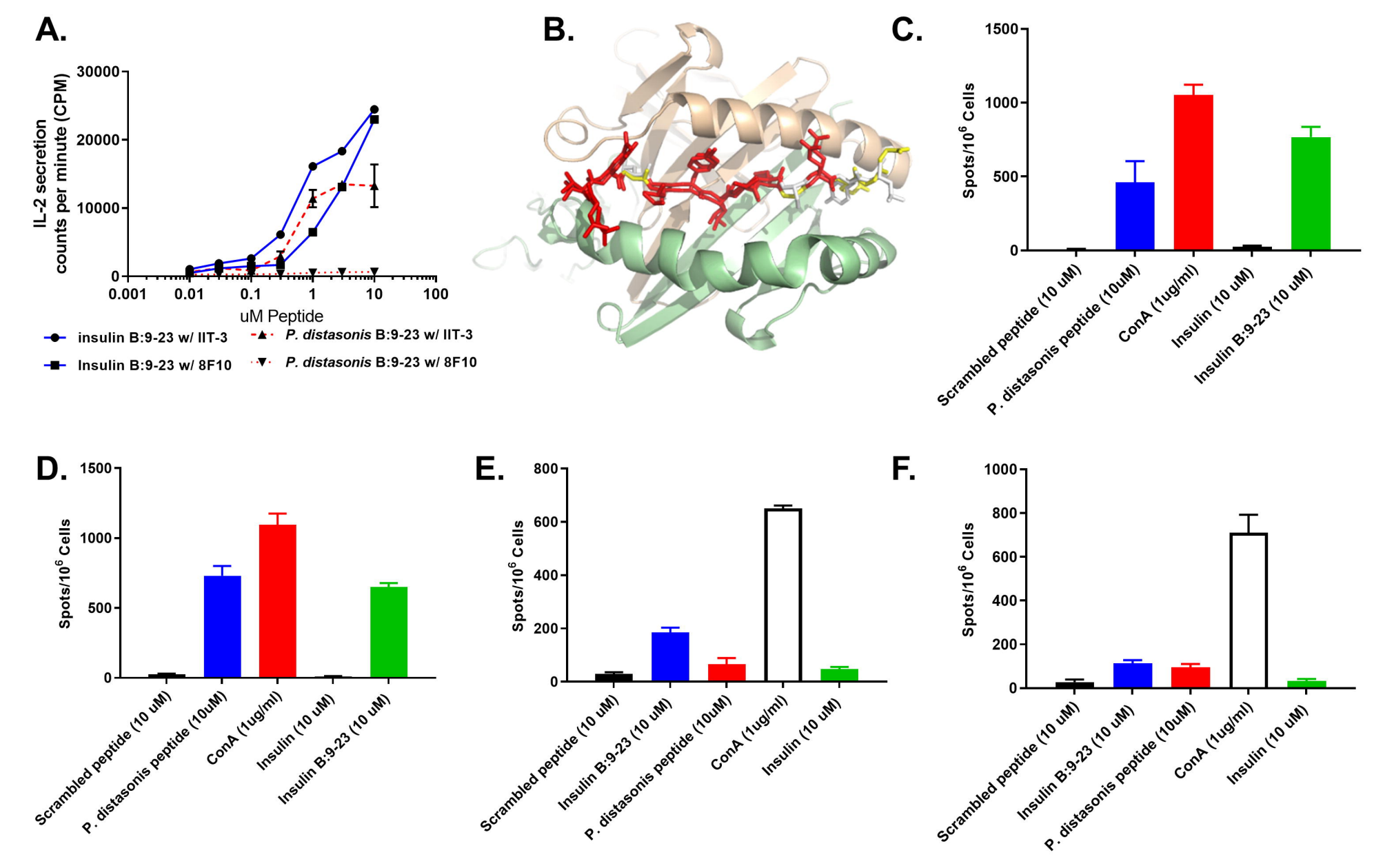
A.
IL-2 secretion counts per minute (CPM)
30000
20000
10000
0
0.001
0.01
0.1
1
10
100
uM Peptide
insulin B:9-23 w/ IIT-3
Insulin B:9-23 w/ 8F10
P. distasonis B:9-23 w/ IIT-3
P. distasonis B:9-23 w/ 8F10
B.
C.
Spots/10^6 Cells
1500
1000
500
0
Scrambled peptide (10 uM)
P. distasonis peptide (10uM)
ConA (1ug/ml)
Insulin (10 uM)
Insulin B:9-23 (10 uM)
D.
Spots/10^6 Cells
1500
1000
500
0
Scrambled peptide (10 uM)
P. distasonis peptide (10uM)
ConA (1ug/ml)
Insulin (10 uM)
Insulin B:9-23 (10 uM)
E.
Spots/10^6 Cells
800
600
400
200
0
Scrambled peptide (10 uM)
Insulin B:9-23 (10 uM)
P. distasonis peptide (10uM)
ConA (1ug/ml)
Insulin (10 uM)
F.
Spots/10^6 Cells
1000
800
600
400
200
0
Scrambled peptide (10 uM)
Insulin B:9-23 (10 uM)
P. distasonis peptide (10uM)
ConA (1ug/ml)
Insulin (10 uM)

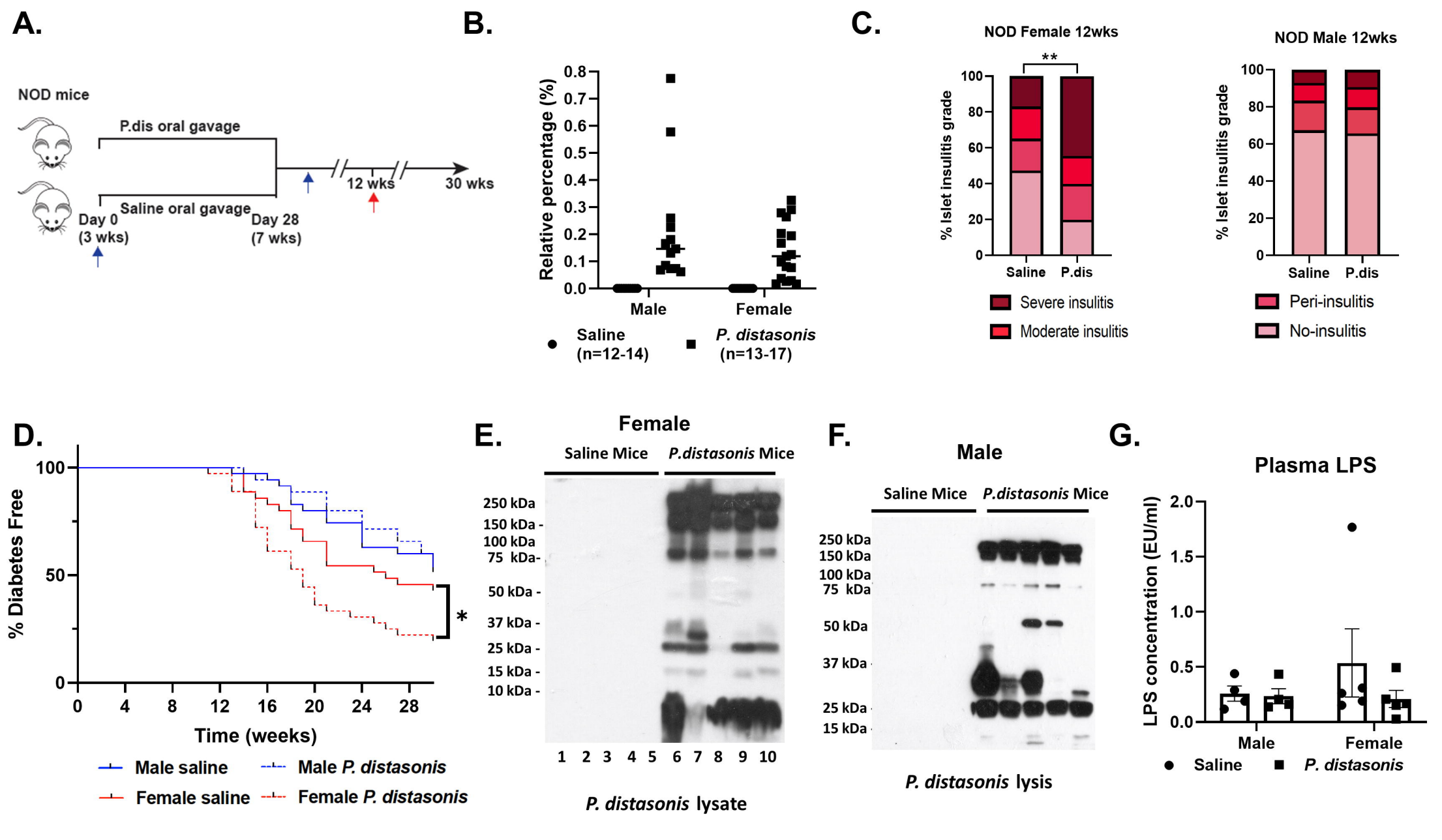
A.
NOD mice
P.dis oral gavage
Saline oral gavage
Day 0
(3 wks)
Day 28
(7 wks)
12 wks
30 wks
B.
Relative percentage (%)
0.8
0.7
0.6
0.5
0.4
0.3
0.2
0.1
0.0
Male
Female
Saline
(n=12-14)
P. distasonis
(n=13-17)
C.
NOD Female 12wks
**
% Islet insulitis grade
100
80
60
40
20
0
Saline
P.dis
Severe insulitis
Moderate insulitis
NOD Male 12wks
% Islet insulitis grade
Saline
P.dis
Peri-insulitis
No-insulitis
D.
% Diabetes Free
100
50
0
0
4
8
12
16
20
24
28
Time (weeks)
*
Male saline
Male P. distasonis
Female saline
Female P. distasonis
E.
Female
Saline Mice
P.distasonis Mice
250 kDa
150 kDa
100 kDa
75 kDa
50 kDa
37 kDa
25 kDa
15 kDa
10 kDa
1 2 3 4 5 6 7 8 9 10
P. distasonis lysate
F.
Male
Saline Mice
P.distasonis Mice
250 kDa
150 kDa
100 kDa
75 kDa
50 kDa
37 kDa
25 kDa
15 kDa
P. distasonis lysis
G.
Plasma LPS
LPS concentration (EU/ml)
2.0
1.5
1.0
0.5
0.0
Male
Female
Saline
P. distasonis

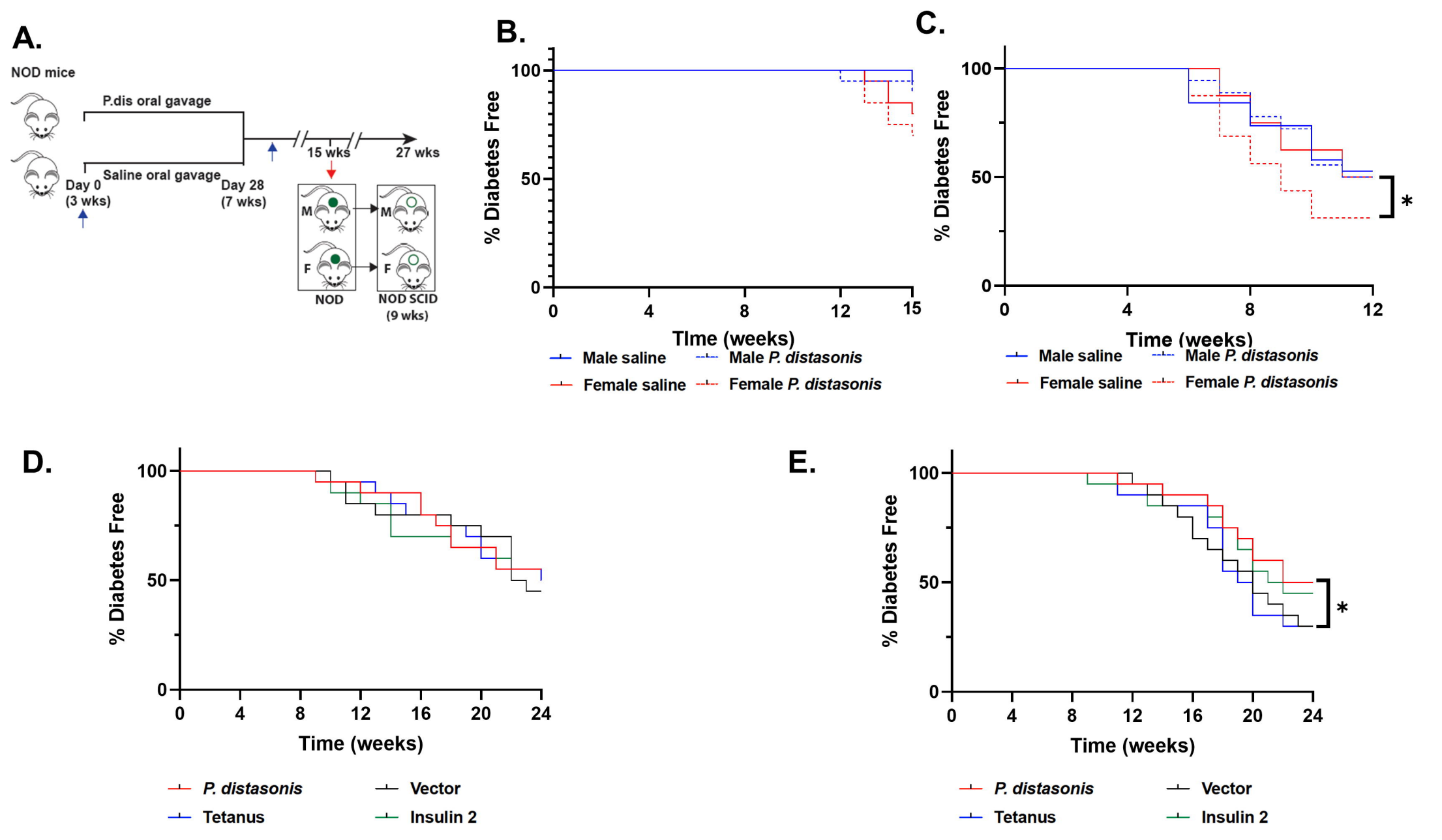
A.
NOD mice
P.dis oral gavage
Saline oral gavage
Day 0
(3 wks)
Day 28
(7 wks)
15 wks
27 wks
M
F
NOD
NOD SCID
(9 wks)
B.
% Diabetes Free
100
50
0
0
4
8
12
15
TIme (weeks)
Male saline
Male P. distasonis
Female saline
Female P. distasonis
C.
% Diabetes Free
100
50
0
0
4
8
12
Time (weeks)
*
Male saline
Male P. distasonis
Female saline
Female P. distasonis
D.
% Diabetes Free
100
50
0
0
4
8
12
16
20
24
Time (weeks)
P. distasonis
Vector
Tetanus
Insulin 2
E.
% Diabetes Free
100
50
0
0
4
8
12
16
20
24
Time (weeks)
*
P. distasonis
Vector
Tetanus
Insulin 2

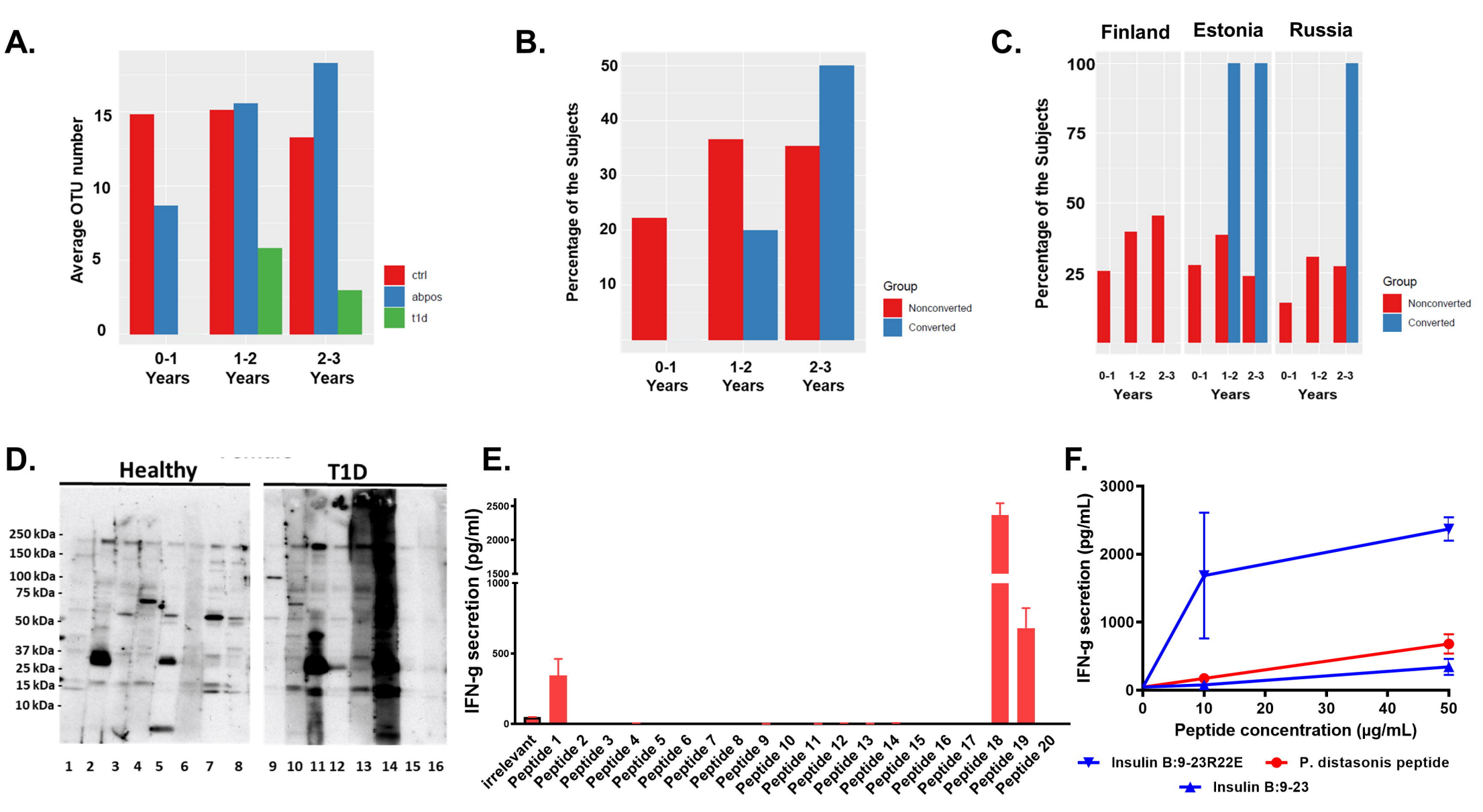
A.
Average OTU number
0
5
10
15
0-1 Years
1-2 Years
2-3 Years
ctrl
abpos
t1d
B.
Percentage of the Subjects
10
20
30
40
50
0-1 Years
1-2 Years
2-3 Years
Group
Nonconverted
Converted
C.
Finland
Estonia
Russia
Percentage of the Subjects
25
50
75
100
0-1 1-2 2-3
Years
Group
Nonconverted
Converted
D.
Healthy
T1D
250 kDa
150 kDa
100 kDa
75 kDa
50 kDa
37 kDa
25 kDa
15 kDa
10 kDa
1 2 3 4 5 6 7 8
9 10 11 12 13 14 15 16
E.
IFN-g secretion (pg/ml)
0
500
1000
1500
2000
2500
irrelevant
Peptide 1
Peptide 2
Peptide 3
Peptide 4
Peptide 5
Peptide 6
Peptide 7
Peptide 8
Peptide 9
Peptide 10
Peptide 11
Peptide 12
Peptide 13
Peptide 14
Peptide 15
Peptide 16
Peptide 17
Peptide 18
Peptide 19
Peptide 20
F.
IFN-g secretion (pg/mL)
0
1000
2000
3000
0 10 20 30 40 50
Peptide concentration (µg/mL)
Insulin B:9-23R22E
P. distasonis peptide
Insulin B:9-23

**A.**

**>EEY82194.1 hypoxanthine phosphoribosyltransferase [Bacteroides sp. 2_1_33B]**

MLN**RILVELLYLVCSEYL**NHNSRCLGFYSAYKCITNFGMLLHFFVHRRKSCTFVPSKTERFMDRIRLKDKEFELFIPESDIQAAIAKMAVQIKADVEGKNPLFVGVLNGAFMFVAELMRE
LDVPYELTFARYSSYQGTSSTGILNEIMPVQADIRGRMVILLEDIIDTGFTMSYVMEKLRSEGAADVRLATMLFKPESLKCELTPDYVGLQIPADFIVGHGLDYDELGRSYKDIYKVVE

**>EEU50637.1 hypoxanthine phosphoribosyltransferase [Parabacteroides sp. D13]**

MLN**RILVELLYLVCSEYL**NHNSRCLGFYSAYKCITNFGMLLHFFVHRRKSCTFVPSKTERFMDRIRLKDKEFELFIPESDIQAAIAKMAVQIKADVEGKNPLFVGVLNGAFMFVAELMRE
LDVPYELTFARYSSYQGTSSTGILNEIMPVQADICGRMVILLEDIIDTGFTMSYVMEKLRSEGAADVRLATMLFKPESLKCELTPDYVGLQIPADFIVGHGLDYDELGRSYKDIYKVVE

**B.**

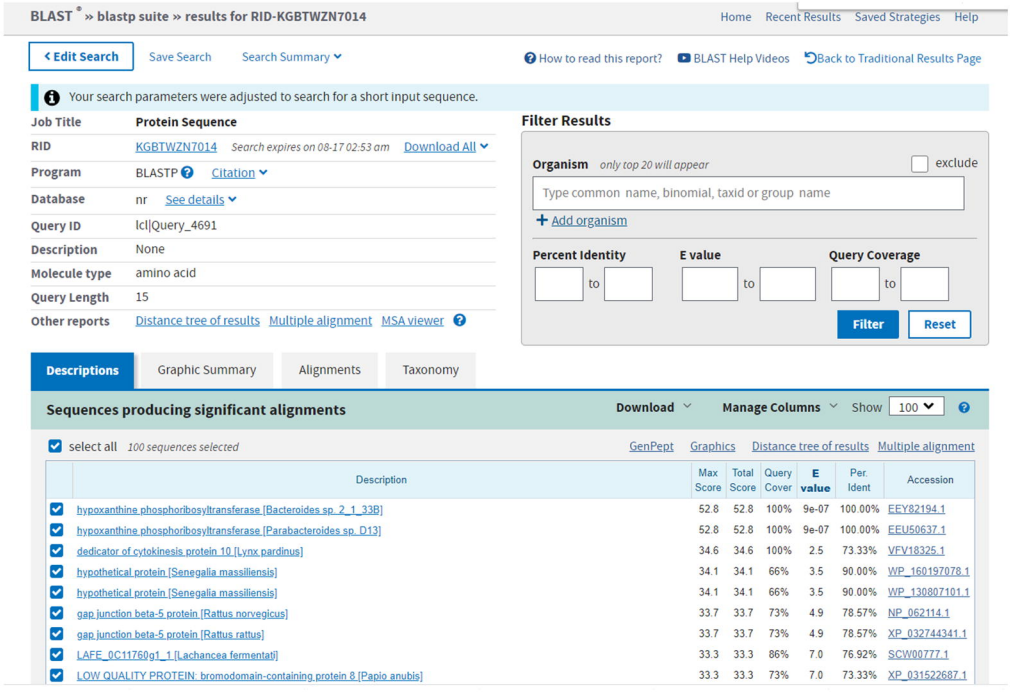


**C.**

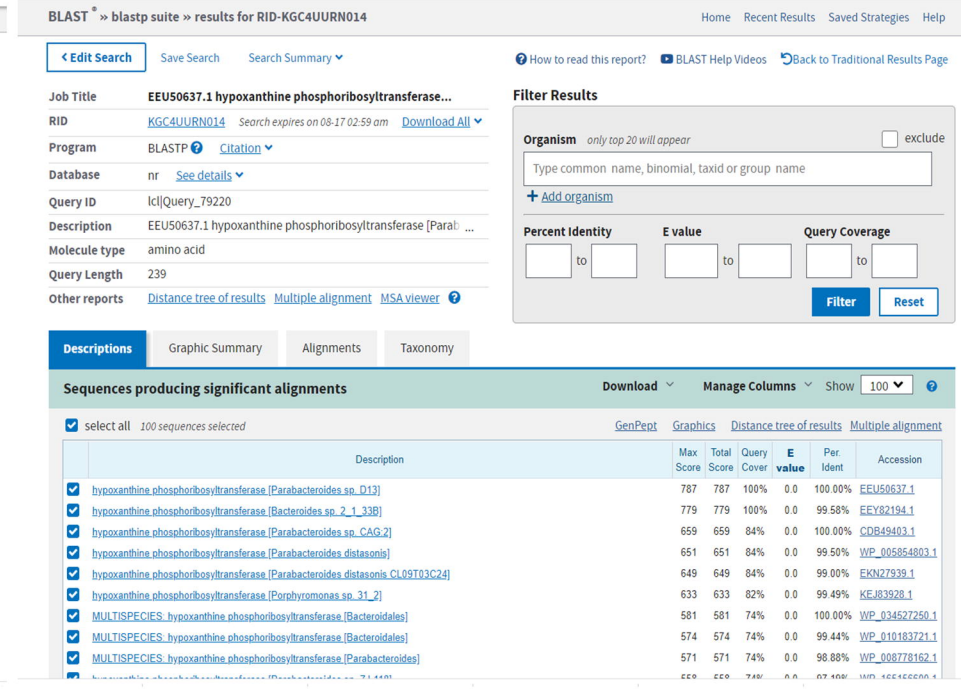

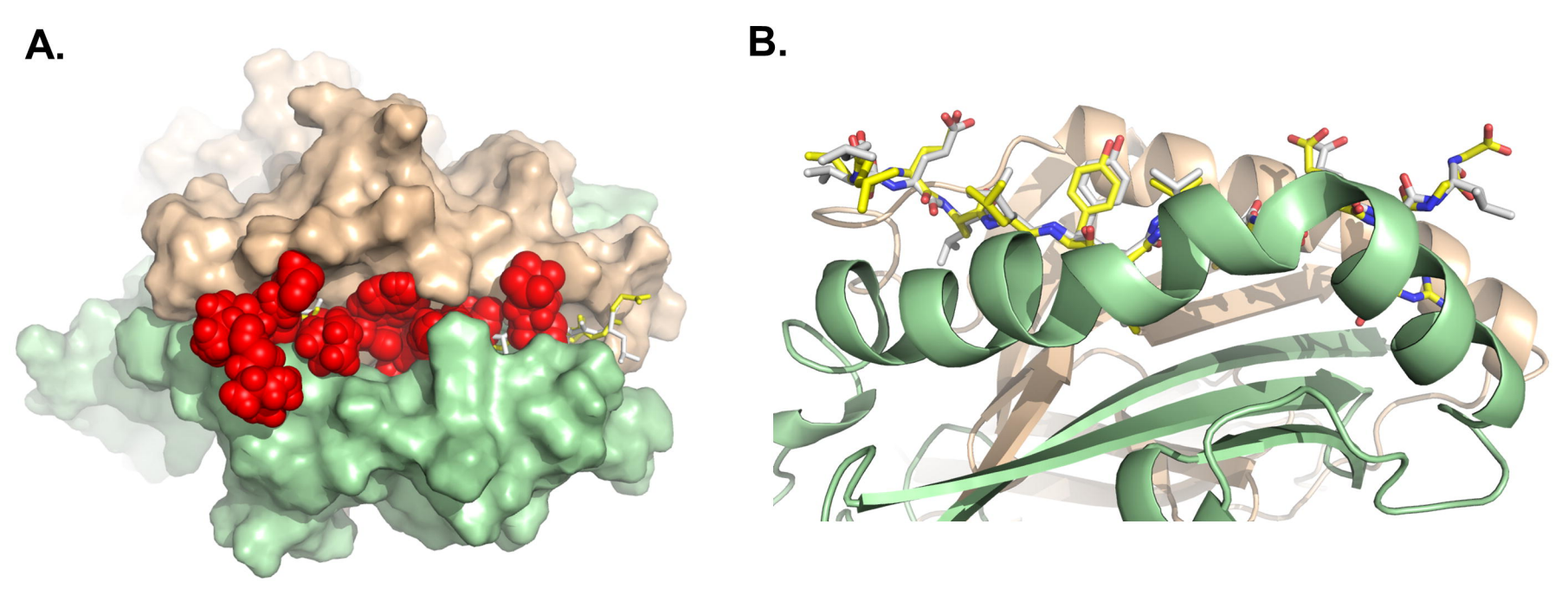
A.
B.

A.

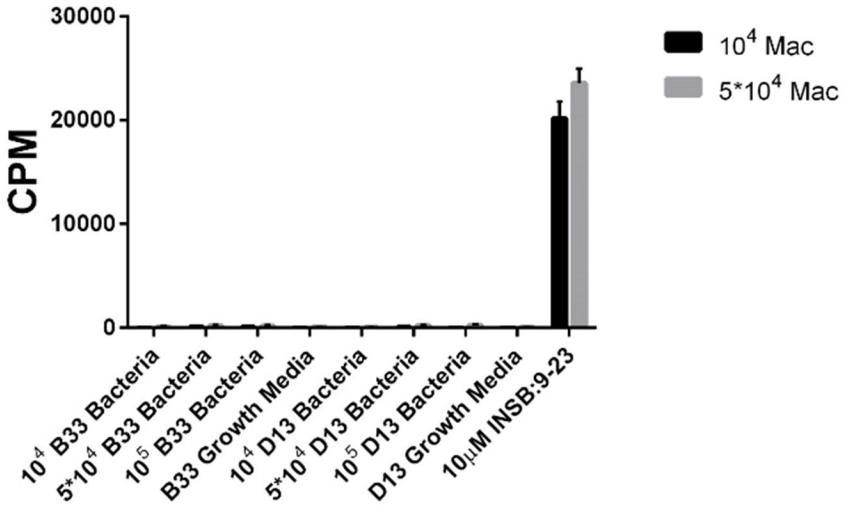
Peritoneal Mac Presentation to IIT-3
CPM
30000
20000
10000
0
10^4 Mac
5*10^4 Mac
10^4 B33 Bacteria
5*10^4 B33 Bacteria
10^5 B33 Bacteria
B33 Growth Media
10^4 D13 Bacteria
5*10^4 D13 Bacteria
10^5 D13 Bacteria
D13 Growth Media
10μM INSB:9-23

B.

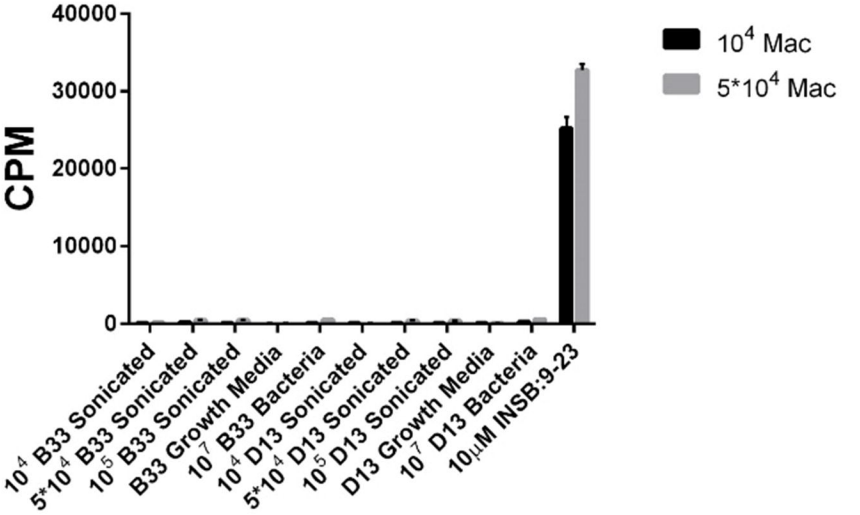
Peritoneal Mac Presentation to IIT-3
CPM
40000
30000
20000
10000
0
10^4 Mac
5*10^4 Mac
10^4 B33 Sonicated
5*10^4 B33 Sonicated
10^5 B33 Sonicated
B33 Growth Media
10^7 B33 Bacteria
10^4 D13 Sonicated
5*10^4 D13 Sonicated
10^5 D13 Sonicated
D13 Growth Media
10^7 D13 Bacteria
10μM INSB:9-23

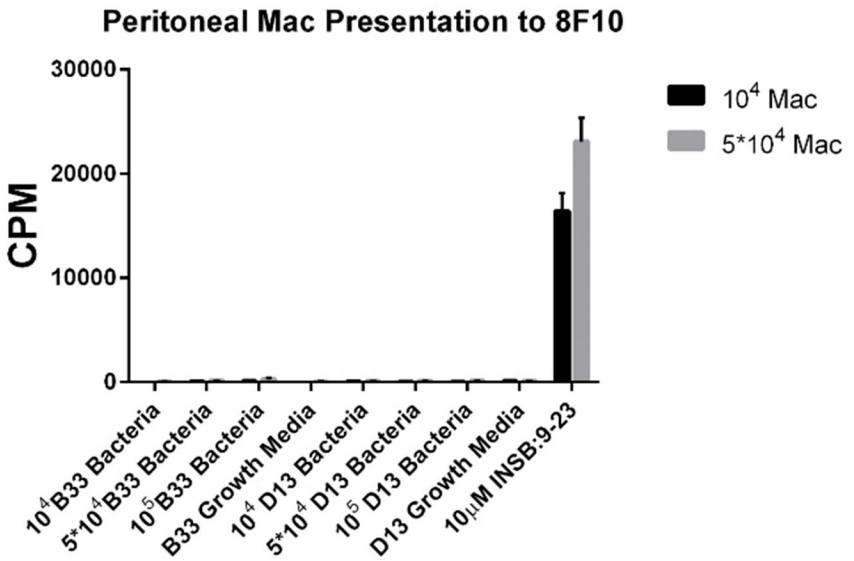
Peritoneal Mac Presentation to 8F10
CPM
30000
20000
10000
0
10^4 Mac
5*10^4 Mac
10^4 B33 Bacteria
5*10^4 B33 Bacteria
10^5 B33 Bacteria
B33 Growth Media
10^4 D13 Bacteria
5*10^4 D13 Bacteria
10^5 D13 Bacteria
D13 Growth Media
10μM INSB:9-23

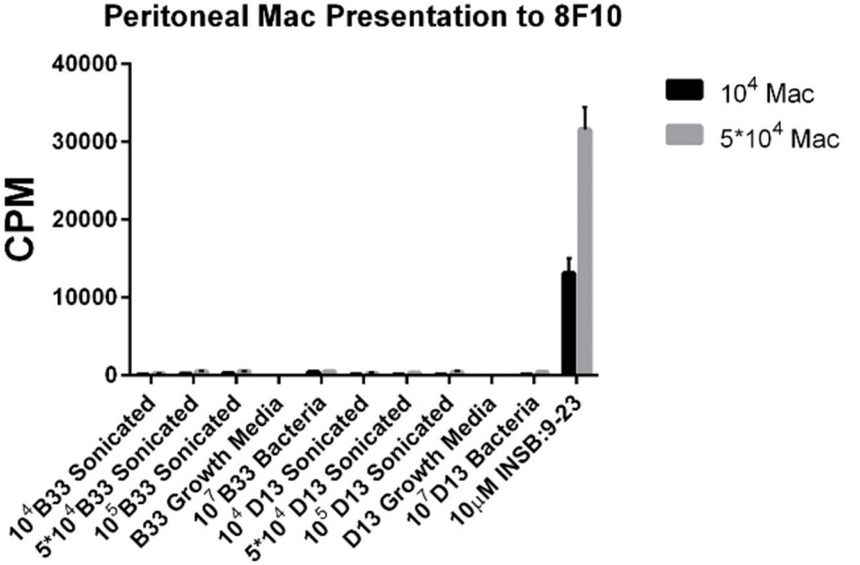
Peritoneal Mac Presentation to 8F10
CPM
40000
30000
20000
10000
0
10^4 Mac
5*10^4 Mac
10^4 B33 Sonicated
5*10^4 B33 Sonicated
10^5 B33 Sonicated
B33 Growth Media
10^7 B33 Bacteria
10^4 D13 Sonicated
5*10^4 D13 Sonicated
10^5 D13 Sonicated
D13 Growth Media
10^7 D13 Bacteria
10μM INSB:9-23

C.

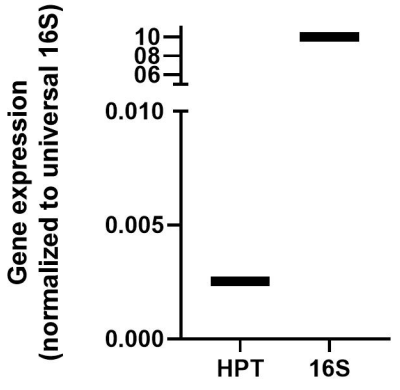
Gene expression
(normalized to universal 16S)
10
08
06
0.010
0.005
0.000
HPT
16S

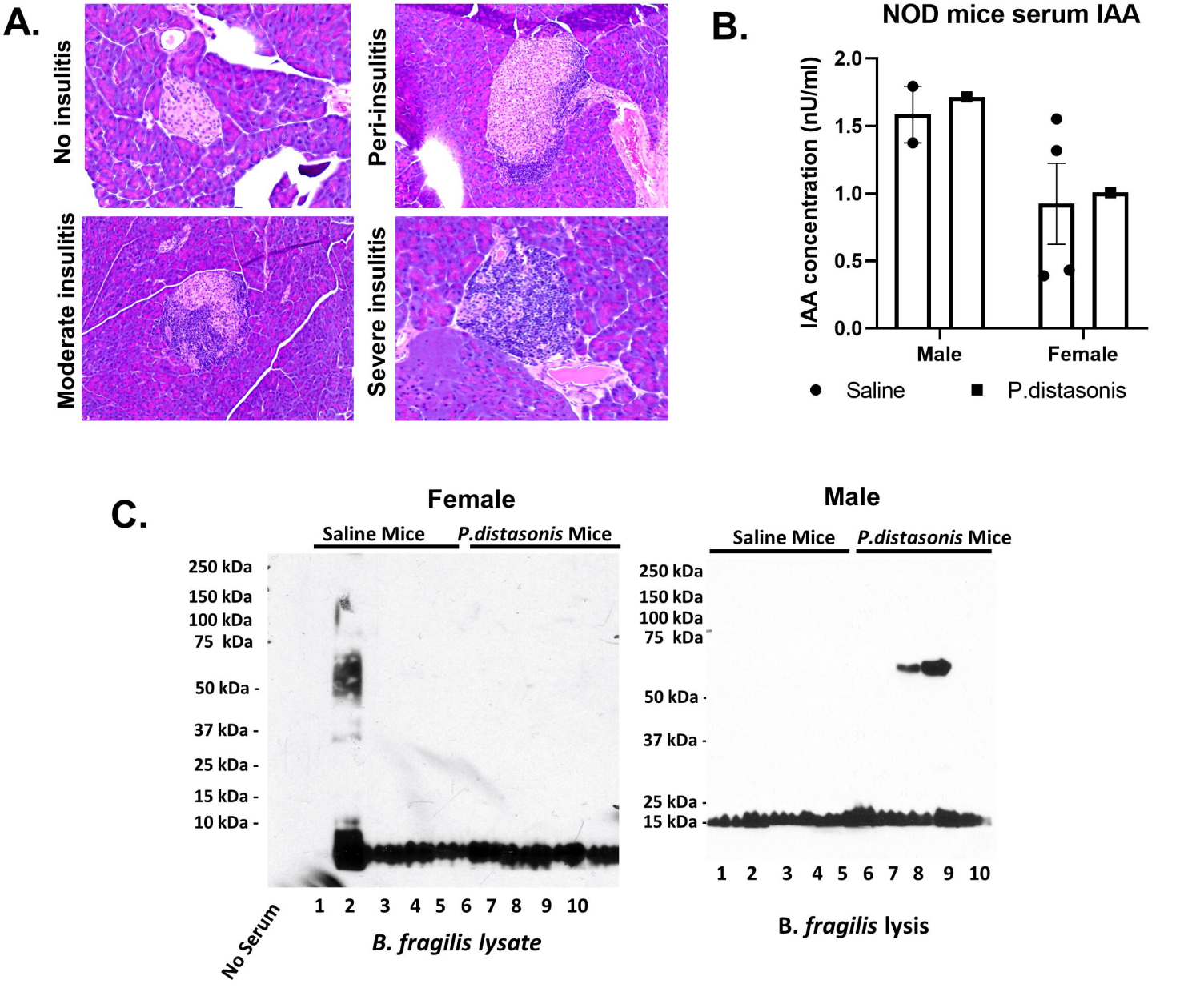
A.
No insulitis
Peri-insulitis
Moderate insulitis
Severe insulitis
B.
NOD mice serum IAA
IAA concentration (nU/ml)
2.0
1.5
1.0
0.5
0.0
Male
Female
Saline
P.distasonis
C.
Female
Saline Mice
P.distasonis Mice
250 kDa
150 kDa
100 kDa
75 kDa
50 kDa
37 kDa
25 kDa
15 kDa
10 kDa
1 2 3 4 5 6 7 8 9 10
No Serum
B. fragilis lysate
Male
Saline Mice
P.distasonis Mice
250 kDa
150 kDa
100 kDa
75 kDa
50 kDa
37 kDa
25 kDa
15 kDa
1 2 3 4 5 6 7 8 9 10
B. fragilis lysis